Estimating the instantaneous velocity of randomly moving target swarms in a stratified ocean waveguide by Doppler analysis

Estimating the instantaneous velocity of randomly moving target swarms in a stratified ocean waveguide by Doppler analysis

Ioannis Bertsatos and Nicholas C. Makris[a)]
Massachusetts Institute of Technology, Mechanical Engineering, 77 Massachusetts Avenue, Cambridge, Massachusetts 02139

(Received 13 May 2010; revised 9 December 2010; accepted 22 January 2011)

Doppler analysis has been extensively used in active radar and sonar sensing to estimate the speed and direction of a *single* target within an imaging system resolution cell following deterministic theory. For target swarms, such as fish and plankton in the ocean, and raindrops, birds and bats in the atmosphere, multiple randomly moving targets typically occupy a single resolution cell, making single-target theory inadequate. Here, a method is developed for simultaneously estimating the instantaneous mean velocity and position of a group of randomly moving targets within a resolution cell, as well as the respective standard deviations across the group by Doppler analysis in free-space and in a stratified ocean waveguide. While the variance of the field scattered from the swarm is shown to typically dominate over the mean in the range-velocity ambiguity function, cross-spectral coherence remains and maintains high Doppler velocity and position resolution even for coherent signal processing algorithms such as the matched filter. For pseudo-random signals, the mean and variance of the swarms' velocity and position can be expressed in terms of the first two moments of the measured range-velocity ambiguity function. This is shown analytically for free-space and with Monte-Carlo simulations for an ocean waveguide.
 [DOI: 10.1121/1.3557039]

PACS number(s): 43.30.Es, 43.30.Gv, 43.30.Sf, 43.30.Vh [DRD] Pages: 84–101

I. INTRODUCTION

Doppler analysis has been extensively used in active radar and sonar sensing to estimate the speed and direction of a *single* target within an imaging system resolution cell based on coherent mean field theory.[1,2] For target swarms, such as fish, plankton, and Autonomous Underwater Vehicles (AUVs) in the ocean, and raindrops, birds, and bats in the atmosphere, multiple randomly moving targets typically occupy a single resolution cell, making single-target theory inadequate. The heuristic assumption, typically made for target swarms in both radar and sonar, is that the mean velocity of the group can be approximated by taking the first moment of the range-Doppler ambiguity function along the velocity axis.[3–5] Here, we prove that this approach leads to accurate estimates of mean group velocity by applying scattering theory to a group of randomly moving targets within a resolution cell. We also show that while the variance of the field scattered from the swarm typically dominates over the mean in the range-velocity ambiguity function for swarm extents greatly exceeding the wavelength, cross-spectral coherence remains and maintains high Doppler velocity and position resolution even for coherent signal processing algorithms such as the matched filter which were originally developed for mean field analysis. Estimators are derived for the mean instantaneous velocity and position of the random target group within a resolution cell, as well as the respective *standard deviations* for long-range acoustic remote sensing system in both free-space and in a stratified ocean waveguide. Domination of the variance in the scattered field intensity has previously been shown to occur for the special case of large aggregations of immobile targets where no Doppler shifts occur.[6]

The application of Doppler sonar to determine the velocity of moving target swarms in the ocean, such as fish and plankton, has been limited to relatively short range (tens to hundreds of meters) and effectively free-space scenarios[7–13] because the low Mach numbers of the swarms make higher frequency signals (tens to hundreds of kilohertzs) more convenient for resolving Doppler shifts. Higher frequency signals, however, suffer increased attenuation and so are limited to shorter ranges. Here, we investigate the possibility of determining Doppler velocity at much greater ranges by using low frequency pseudo-random signals that suffer low attenuation and have high range and Doppler resolution in both free-space and in an ocean waveguide. As range increases in ocean sensing applications beyond the water depth, waveguide propagation ensues. The problem of scattering from a single object moving in a waveguide is far more complicated than that of one moving in free-space. It is known, for example, that for a waveguide supporting N modes, N^2 Doppler shifts as opposed to the single shift will occur in free-space for the same motion.[14] We show here that by applying a statistical formulation to the even more complicated problem of sensing multiple randomly moving targets in an ocean waveguide within a single imaging system resolution cell, the analysis can be greatly simplified.

For appropriate signal design, such as pseudo-random signals, we find that the mean and variance of the swarm's velocity and position can be expressed in terms of the first two moments of the measured range-velocity ambiguity function. This is derived analytically for free-space and demonstrated

a)Author to whom correspondence should be addressed. Electronic mail: makris@mit.edu

with Monte-Carlo simulations for an ocean waveguide. We refer to simultaneous estimation of the group's velocity and position from ambiguity surface moments as the Moment Method. Simultaneous estimates of the mean velocity and position are also obtained by finding the velocity and position that corresponds to the peak of the ambiguity function's expected square magnitude, which we refer to as the Peak Method. We show that estimates of the mean velocity obtained via the Moment Method are at least as accurate as estimates based on the Peak Method. For active sensing of a single deterministic target in a waveguide where N^2 Doppler shifts occur, it has been shown that a relatively accurate estimate of the target velocity can be obtained from the Doppler-shifted spectrum of its scattered field.[14,15] Here, we show that, for a group of random targets within a resolution cell, accurate simultaneous estimates can be obtained for the instantaneous velocity and position means of the group, as well as their standard deviations through the Moment Method.

In Sec. II and the Appendixes, we derive analytic expressions for the statistical moments of the field scattered from a single moving target in free-space or a stratified range-independent waveguide, given random target velocity and position and arbitrary source spectrum. We then derive the expected value and expected square magnitude of the range-velocity ambiguity function for the total field scattered from a group of random targets. We show in Sec. II that the first and second moments of the ambiguity function's expected square magnitude along constant range and velocity axes in free-space are linear functions of the group's velocity and position means and standard deviations for a pseudo-random signal described in Appendix A known as the Costas sequence. In Sec. III, we demonstrate both the Peak and Moment Methods via illustrative examples in free-space and an ocean waveguide based on field measurements of fish schools from ocean acoustic waveguide remote sensing (OAWRS) experiments.[16]

II. DETERMINING TARGET VELOCITY STATISTICS FROM DOPPLER SHIFT AND SPREAD

We assume a group of N targets are randomly distributed in volume V centered at the origin 0, which is in the far-field of a stationary monostatic source/receiver system at range r, as shown in Fig. 1. We consider a remote sensing sonar platform that consists of a point source collocated with a horizontal receiving array, such as that shown in Fig. 2. We define $\mathbf{u}_q^0$ as the random initial position of the qth target and v_q as the random speed of the qth target *toward* the source/receiver system. We assume that the target positions and velocities are independent and identically distributed (i.i.d.) random variables with probability densities $P_{\mathrm{u}}(\mathbf{u}_q^0)$ and $P_v(v_q)$, which are inherent properties of the target group. We define the means and standard deviations for $\mathbf{u}_q^0$, v_q to be μ_{u}, σ_{u} and μ_v, σ_v, respectively. We also assume that the targets move at low Mach numbers, which is typical for biological scatterers, e.g., fish at velocities of order 1 m/s (Refs. 17–19) and that population densities are not large enough for multiple scattering to be important.[6] As detailed in Appendix B, v_q is defined to be the velocity component parallel to r, which is assumed to be constant during the time necessary for the sound signal to travel through the resolution footprint of the remote sensing system. For simplicity, we assume that all targets have the same scatter function, and for the frequencies considered, they scatter omnidirectionally. We assume that target velocities follow Gaussian probability densities and set the velocity means to correspond to typical fish group swimming speeds, in illustrative examples. A target group is then defined to be migrating by setting the velocity standard deviation to be approximately 10% of the mean velocity. Similarly, a group is defined to be randomly swarming if the velocity standard deviation is much larger than the velocity mean. Targets are assumed to be uniformly distributed within 100 m about a nominal range of 15 km from the remote sensing system. For waveguide examples, we consider the waveguide of Fig. 2, which is representative of continental-shelf environments, and assume that targets are uniformly distributed in depth between 70 and 90 m. For free-space examples, we use the same distributions. Finally, areal number densities are chosen so that acoustic returns from the target groups will stand above the background reverberation,[20] based on the past OAWRS field data from the New Jersey continental shelf and the Gulf of Maine.[16–21] For herring, we then assume an areal number density of 2 fish/m^2, whereas for tuna, we consider imaging a single school consisting of roughly 100 individuals.[20]

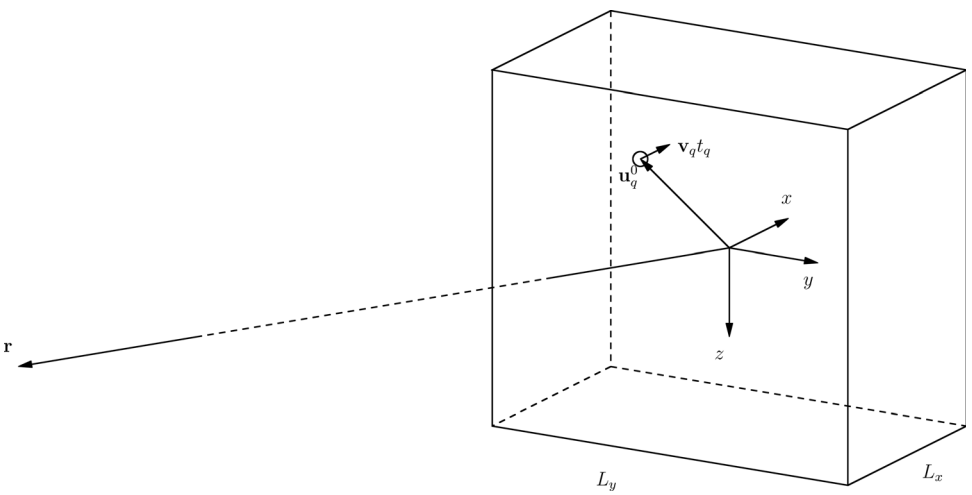

FIG. 1. Sketch of the resolution footprint volume enclosing a target with initial offset u_q^0 from the coordinate system origin and velocity v_q. The variables L_x, L_y, and L_z denote the dimensions of the footprint volume in x, y, and z coordinates, respectively. The position mean and standard deviation are μ_{u}, σ_{u}, while the velocity mean and standard deviation are μ_v, σ_v.

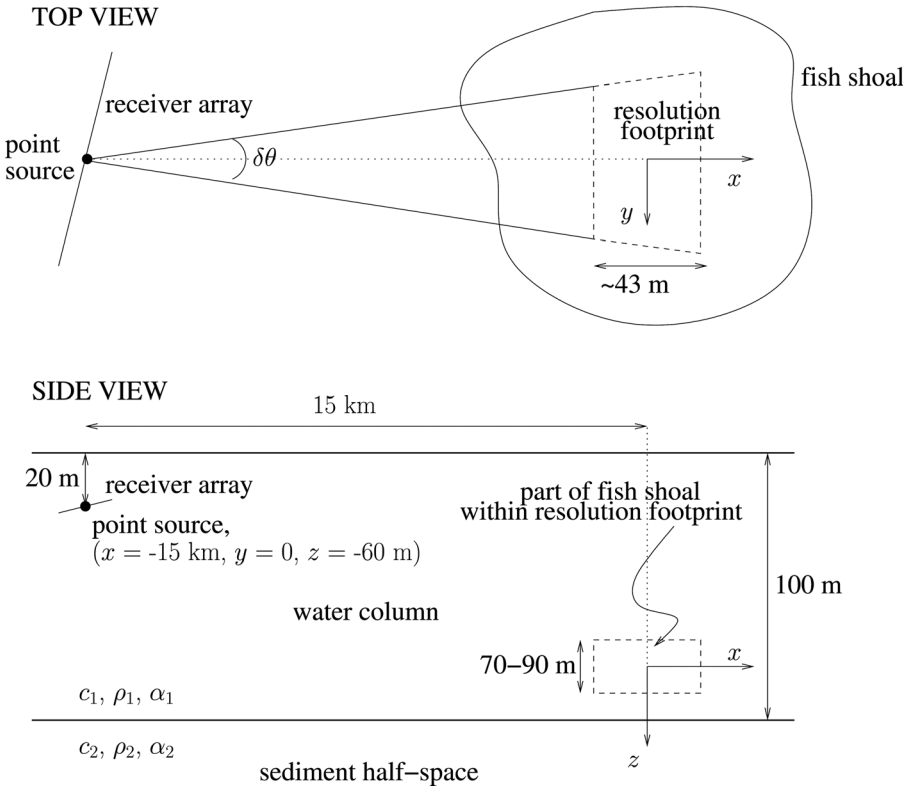

FIG. 2. Sketch of waveguide geometry and sound speed profile. The locations of the fish shoal, the source/receiver imaging system and the resolution footprint with respect to the coordinate system (x, y, and z) are also shown. The coordinate system coincides with that of Fig. 1. The sound speed in the water column is constant, $c_1 = 1500$ m/s, and the sound speed in the sediment half-space is $c_2 = 1700$ m/s. The density ρ_1 and attenuation $\alpha_1$in the water column are 1000 kg/m^3 and 6×10^{-5} dB/λ_1, respectively, where λ_1 is the wavelength in the water column. The sediment half-space has density $\rho_2 = 1900$ kg/m^3 and attenuation $\alpha_2 = 0.8$ dB/λ_2, representative of sand, where λ_2 is the wavelength in the bottom sediment.

In all examples, we employ the specific signal design described in Appendix A, which has center frequency of 1.6 kHz, bandwidth of roughly 20 Hz, velocity resolution of approximately 0.17 m/s, and range resolutions of about 43 m, which is smaller than the range dimension of the targets' spatial distribution. The target distribution scenarios are summarized in Table I, and the source signal and remote sensing system parameters are given in Table II.

A. Free-space

The field scattered from the qth target due to a harmonic source of frequency f and unit amplitude can be written as[14]

$$\Phi_{s,q}(\mathrm{r},t;f) = \frac{S(\bar{f})}{\bar{k}} G(\mathrm{r}|0,\bar{f}) G(0|\mathrm{r},f) e^{-i2\pi\bar{f}t} \times e^{-i2\pi(\bar{f}+f)\hat{\mathrm{i}}_r \cdot \mathrm{u}_q^0/c,} \quad (1)$$

where $\bar{f} \approx f(1 + 2v_q/c)$ is the Doppler-shifted frequency of the scattered field, c is the sound speed in the medium, $S(f)$ is the target's planewave scattering function, and $G(0|\mathrm{r},f)$ is the free-space Green's function between the source and the origin evaluated at frequency f. For a broadband source with dimensionless source function $q(t) \Longleftrightarrow Q(f)$, the scattered field is given by Fourier synthesis as

$$\Psi_{s,q}(\mathrm{r},t) = \int \mathrm{d}f Q(f) \Phi_{s,q}(\mathrm{r},t;f), \quad (2)$$

where $\Longleftrightarrow$ denotes Fourier transform pairs $q(t) = \int Q(f) \times e^{-i2\pi ft} \mathrm{d}f$, $Q(f) = \int q(t) e^{i2\pi ft}\, \mathrm{d}t$.

The ambiguity function is defined as

$$\Psi_{s,q}(\tau,v) = \int_{-\infty}^{\infty} \Psi_{s,q}(\mathrm{r},t) q^*(t-\tau) e^{i2\pi vt} \mathrm{d}t = \int_{-\infty}^{\infty} \Psi_{s,q}(\mathrm{r},f') Q^*(f'-v) e^{-i2\pi(f'-v)\tau} \mathrm{d}f', \quad (3)$$

TABLE I. Target distribution scenarios.

	Case A migrating herring	Case B swarming herring	Case C migrating tuna
Velocity mean, μ_v	0.2 m/s	0 m/s	1.5 m/s
Velocity standard deviation, σ_v	0.025 m/s	0.5 m/s	0.1 m/s
Areal number density, or number of targets	2 fish/m^2		1 school (100 fish)
Position mean, μ_u (from the origin 0, see Figs. 1 and 2)	0		
Target range distribution (from the mean position μ_u)	Uniform, ± 50 m		
Target depth distribution (for waveguide examples, see Fig. 2)	Uniform, 70–90 m		
Target cross-range extent	Exceeds remote sensing system's cross-range resolution		

TABLE II. Remote sensing system properties.

Signal Design	7-pulse Costas sequence (see Appendix A)
Center frequency	1.6 kHz
Bandwidth	≈20 Hz
Range resolution, Δu	≈43 m
Cross-range resolution (at 15 km range)	≈ 100 m
Velocity resolution, Δv	≈ 0.17 m/s
Source/receiver range (from the origin 0, see Figs. 1 and 2)	15 km
Source/receiver depth (for waveguide examples, see Fig. 2)	20 m

where v is the Doppler shift and τ is the time-delay defined such that $\tau = 0$ corresponds to the time instant the signal is transmitted from the source. The ambiguity function has units of pascal per hertz and can also be interpreted in terms of target velocity and position by using the transformations $v = cv/(2f_c)$ and $u = c\tau/2$, where v, u are the target's velocity and position, and f_c is the signal's center frequency. The mean and second moment of the ambiguity function $\Psi_{s,q}(\tau, v)$ are derived analytically in Appendix B1 and are given by

$$\begin{aligned}\langle \Psi_{s,q}(\tau,v)\rangle = &\int_{-\infty}^{\infty} \frac{S(f')}{k'} G(\mathrm{r}|0,f') Q^*(f'-v) e^{-i2\pi(f'-v)\tau} \\ &\times \int G(0|\mathrm{r},f'(1+2v_q/c)^{-1}) Q(f'(1+2v_q/c)^{-1}) \\ &\times U_q(f'\hat{i}_r/c, v_q) P_v(v_q)\mathrm{d}v_q \mathrm{d}f', \end{aligned} \tag{4}$$

$$\begin{aligned}\left\langle |\Psi_{s,q}(\tau,v)|^2 \right\rangle = &\int_{-\infty}^{\infty}\int_{-\infty}^{\infty} \frac{S(f_1)}{k_1} G(\mathrm{r}|0,f_1) Q^*(f_1-v) \\ &\times \frac{S^*(f_2)}{k_2^*} G^*(\mathrm{r}|0,f_2) Q(f_2-v) e^{-i2\pi(f_1-f_2)\tau} \\ &\times \int G(0|\mathrm{r},f_1(1+2v_q/c)^{-1}) Q(f_1(1+2v_q/c)^{-1}) \\ &\times G^*(0|\mathrm{r},f_f(1+2v_q/c)^{-1}) Q^*(f_2(1+2v_q/c)^{-1}) \\ &\times U_q((f_1-f_2)\hat{i}_r/c, v_q) P_v(v_q)\mathrm{d}v_q \mathrm{d}f_1 \mathrm{d}f_2, \end{aligned} \tag{5}$$

where f', f_1, or f_2 correspond to received frequencies, and $Q(f)$is the source spectrum. The variable U_q is defined analytically in Eq. (B4) and is the characteristic function for probability density $P_{\mathrm{u}}(\mathrm{u}_q^0)$, so that it can be interpreted as the Fourier transform of the target's spatial distribution. For the whole group of N targets, we find $|\langle \Psi_s(\tau, v)\rangle|^2 = N^2|\langle \Psi_{s,q}(\tau, v)\rangle|^2$ and (see Appendix B1),

$$\begin{aligned}\left\langle |\Psi_s(\tau,v)|^2 \right\rangle = &N\left\langle |\Psi_{s,q}(\tau,v)|^2 \right\rangle + N(N-1) \\ &\times |\langle \Psi_{s,q}(\tau,v)\rangle|^2. \end{aligned} \tag{6}$$

The expected square magnitude of the ambiguity function is then the sum of (i) a second moment term proportional to N due to scattering from each target, and (ii) a mean-squared term proportional to N^2 due to interaction of the fields scattered from different targets.[22]

For target groups large compared to the wavelength, the source spectrum Q and the targets' spatial spectrum U_q tend to be non-overlapping band-limited functions of frequency whose products tend to zero in Eq. (4), leading to a negligible mean. This is not the case in Eq. (5) where the peaks of Q and U_q overlap because evaluation of U_q at the frequency difference enables cross-spectral coherence. The variance then typically dominates the second moment.[6] This is shown in Fig. 3 for the case A target distribution scenario that represents migrating herring (Table I), given the source signal and remote sensing system parameters in Table II, where we find that the magnitude squared of the expected value of the ambiguity function, $|\langle \Psi_s(\tau, v)\rangle|^2$, is typically about 20 dB smaller than the expected square magnitude of the ambiguity function, $\langle |\Psi_s(\tau, v)|^2\rangle$. From Eq. (6), this means that for this case we would require a 100-fold increase in population density for the magnitude squared of the mean ambiguity function to dominate.

1. Estimating target position and velocity statistics

Equations (4) and (5) cannot typically be evaluated analytically. A significant simplification is however possible in the case of specially designed source signals whose spectra can be approximated as

$$\begin{aligned} Q(f) &= \sum_{n=0}^{M-1} a_n e^{i2\pi(f-f_n)h_n} \sin \mathrm{c}(\pi(f-f_n)T) \\ &\approx \sum_{n=0}^{M-1} a_n e^{i2\pi(f-f_n)h_n} \delta(f-f_n), \end{aligned} \tag{7}$$

where a_n is the coefficient of the nth frequency component, f_n, for $n = 1,2,\ldots,M$ and h_n and T are known constants. Equation (7) is approximately valid, for example, for spectra that consist of a series of windowed harmonic waves, such as the Costas sequence described in Appendix A. For such spectra, the expected square magnitude of the ambiguity function is given by

$$\begin{aligned}\left\langle |\Psi_{s,q}(\tau,v)|^2 \right\rangle = &\sum_{n=0}^{M-1}\sum_{m=0}^{M-1}\sum_{i=0}^{M-1}\sum_{j=0}^{M-1} a_n^* a_m a_l a_j^* \left[\frac{S(f_n+v)}{2\pi(f_n+v)/c}\right] \\ &\times \left[\frac{S^*(f_l+v)}{2\pi(f_l+v)/c}\right] \times G(\mathrm{r}|0,f_n+v) \\ &\times G^*(\mathrm{r}|0,f_l+v) G(0|\mathrm{r},f_m) G^*\left(0|\mathrm{r},\frac{f_l+v}{f_n+v}f_m\right) \\ &\times \delta\left(\frac{f_l+v}{f_n+v}f_m - f_j\right) U_q\left(\left[f_n+f_m-f_l-\frac{f_l+v}{f_n+v}f_m\right]\right. \\ &\left.\times \hat{i}_r/(2c), 0\right) \times e^{-i2\pi(f_n-f_l)\tau} P_v\left(\frac{c}{2}\left[\frac{f_n+v}{f_m}-1\right]\right) \end{aligned} \tag{8}$$

When the dimensions of the swarm are much larger than the acoustic wavelength, the first two moments of Eq. (8) along constant Doppler shift v and constant time-delay τ axes can be analytically expressed in terms of the targets' position and velocity first and second statistical moments (see Appendix B1). Taking moments along a constant-τ axis,

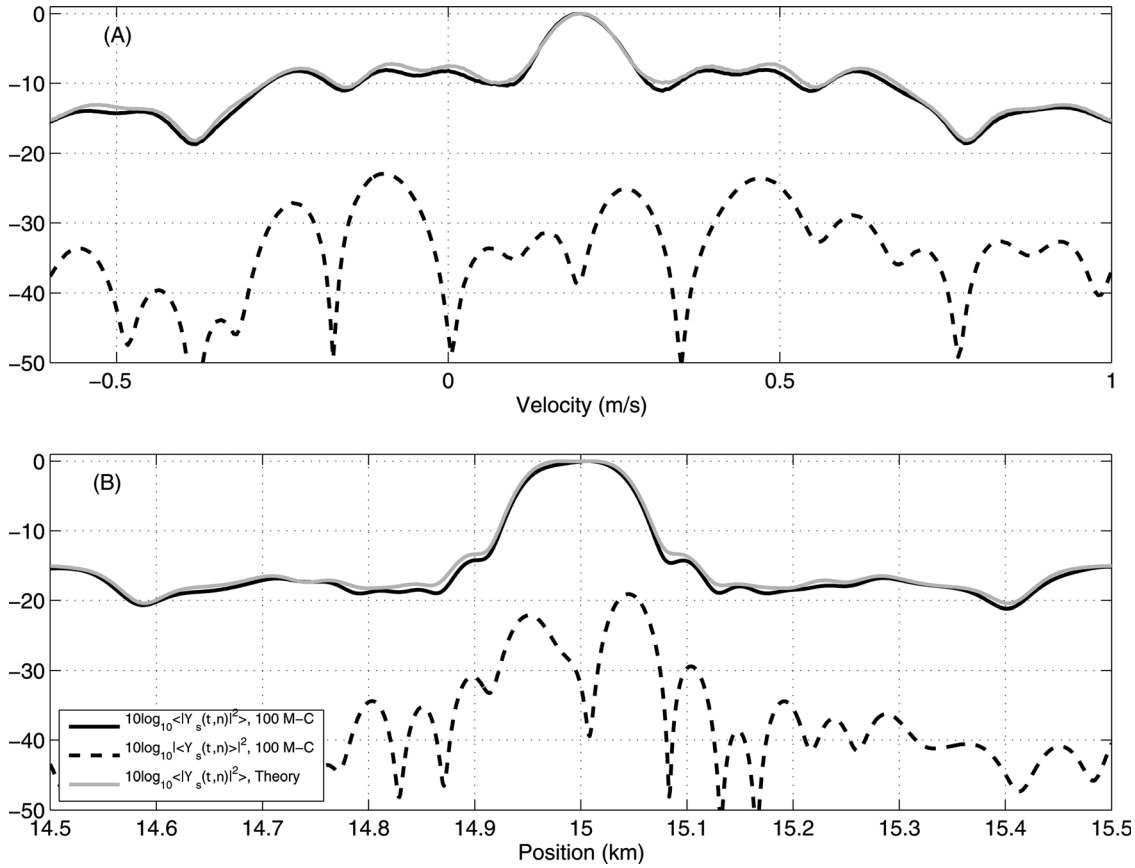

FIG. 3. Free-space. $10\log_{10}|\langle\Psi(\tau,v)\rangle|^2$ (black dashed line) and $10\log_{10}\langle|\Psi(\tau,v)|\rangle^2$ (black solid line) via 100 Monte-Carlo simulations for the field scattered from a random aggregation of targets following the case A scenario described in Table I. The source signal and remote sensing system parameters are given in Table II. $10\log_{10}$ of the expected square magnitude of the ambiguity function, based on the analytical expressions of Eqs. (4) and (5), and (6) is also shown (gray line) and is found to be in good agreement with the Monte-Carlo result. The variance of the ambiguity function dominates the total intensity and the magnitude squared of the ambiguity function's expected value is negligible.

$$v_1 = \int v\left\langle|\Psi_{s,q}(\tau,v)|^2\right\rangle \mathrm{d}v \approx b_1\left\{\left[\sum_{n=0}^{M-1}\sum_{m=0}^{M-1}\frac{2f_m}{c}(f_m-f_n)\right] + \left[M\sum_{m-0}^{M-1}\left(\frac{2f_m}{c}\right)^2\right]\mu_v\right\} \approx c_1 + d_1\mu_v, \tag{9a}$$

$$v_2 = \int v^2\left\langle|\Psi_{s,q}(\tau,v)|^2\right\rangle \mathrm{d}v \approx b_1\left\{\left[\sum_{n=0}^{M-1}\sum_{m=0}^{M-1}\frac{2f_m}{c}(f_m-f_n)^2\right] + \left[\sum_{n=0}^{M-1}\sum_{m=0}^{M-1}2\left(\frac{2f_m}{c}\right)^2(f_m-f_n)\right]\mu_v + \left[M\sum_{m=0}^{M-1}\left(\frac{2f_m}{c}\right)^3\right](\mu_v^2+\sigma_v^2)\right\} \approx c_2 + d_2\mu_v + e_2(\mu_v^2+\sigma_v^2), \tag{9b}$$

TABLE III. Coefficients of Eq. (9).

c_1	d_1	c_2	d_2	e_2
0.0156	2.1334	0.5822	0.1333	4.5512

where the ambiguity function has been normalized so that $\int\langle|\Psi_{s,q}(\tau,v)|^2\rangle \mathrm{d}v = 1$. The coefficient b_1 is given by

$$b_1 = \left[M\sum_{m=0}^{M-1}\frac{2f_m}{c}\right]^{-1}. \tag{10}$$

The coefficients c_1, d_1, c_2, d_2, and e_2 can be calculated analytically, given a specific signal design, and then used to provide estimates of the target's mean velocity and its standard deviation given measurements of v_1 and v_2. For the purposes of this paper, we employ the Costas sequence design detailed in Appendix A that satisfies Eq. (7), and for which the coefficients are given in Table III. In the illustrative examples of Sec. III A, we assume the form of Eq. (9) holds and use it to estimate the velocity means and standard deviations. Estimates obtained via the Moment Method in Sec. III A are found to be very accurate, with errors typically smaller than 10%.

Similarly, for the moments of the expected square magnitude of the ambiguity function over time-delay τ, we find

$$\tau_1 = \int \tau \left\langle |\Psi_{s,q}(\tau, v)|^2 \right\rangle \mathrm{d}\tau$$
$$= (r + \hat{\mathrm{i}}_r \cdot \mu_{\mathrm{u}}) \frac{1}{c} \sum_{n=0}^{M-1} \sum_{m=0}^{M-1} d_{n,m}, \tag{11a}$$

$$\tau_2 = \int \tau^2 \left\langle |\Psi_{s,q}(\tau, v)|^2 \right\rangle \mathrm{d}\tau$$
$$= (|\hat{\mathrm{i}}_r \cdot \sigma_{\mathrm{u}}|^2 + |r + \hat{\mathrm{i}}_r \cdot \mu_{\mathrm{u}}|^2) \frac{2}{c^2} \sum_{n=0}^{M-1} \sum_{m=0}^{M-1} d_{n,m}, \tag{11b}$$

where r is the range from the monostatic source/receiver position to the center of the resolution footprint, and the ambiguity function has again been normalized so that $\int \langle |\Psi_{s,q}(\tau, v)|^2 \rangle \mathrm{d}\tau = 1$. The coefficients $d_{n,m}$ are given by

$$d_{n,m} = P_v\left(\frac{c}{2}\left[\frac{f_n + v}{f_m} - 1\right]\right). \tag{12}$$

Equation (11) shows that the first two moments of the ambiguity function's expected square magnitude along a constant Doppler shift axis are linearly related to the first two moments of the target swarm's position. Note that as long as the absolute value of the mean position estimate is less than or equal to the length scale of the resolution footprint, then for practical purposes the targets have been accurately localized.

B. Waveguide

As in Sec. II A, we assume a group of N targets is randomly distributed within volume V in the far-field of a monostatic source/receiver system in a stratified range-independent waveguide. We also assume that targets scatter omnidirectionally for the frequencies considered. Under these conditions, the field scattered from the qth target, due to a harmonic source at angular frequency Ω, can be found by adapting Eq. (59) of Ref. 14 to account for the case of a monostatic ($r_0 = r$), stationary ($v_0 = v = 0$) system and for the change of the coordinate system origin from the target centroid to the center of the resolution footprint

$$\Phi_{s,q}(\mathrm{r}, t; \Omega) = 4\pi \sum_l \sum_m \frac{\mathrm{S}(\omega_{m,l,q})}{k(\omega_{m,l,q})} \Phi_{s,q}^{l,m}(\mathrm{r}, \Omega, \omega_{m,l,q}) e^{-i\omega_{m,l,q} t}, \tag{13}$$

where $\omega_{m,l,q} = \Omega + v_q[\xi_l(\Omega) + \xi_m(\Omega)]$ is the Doppler-shifted frequency due to target motion, ξ is the wavenumber, $S(\omega)$ is the target's planewave scattering function, l and m are indices corresponding to the incoming and outgoing modes, respectively, and the variable $\Phi_{s,q}^{l,m}$ describing propagation to and from the target is defined explicitly in Eq. (B30). Note that both the scattering function and the wavenumber are evaluated at the Doppler-shifted frequency $\omega_{m,l,q}$ due to modal propagation. The mean and second moment of the ambiguity function of the back-scattered field are derived analytically in Appendix B2 and are given by

$$\left\langle \Psi_{s,q}(\tau, v) \right\rangle = \frac{1}{\pi} \int_{-\infty}^{\infty} \frac{S(\omega')}{k(\omega')} Q^*(\omega' - 2\pi v) e^{-i(\omega' - 2\pi v)\tau}$$
$$\times \int \sum_l \sum_m Q(\omega'(1 + v_q(1/v_l^G + 1/v_m^G))^{-1})$$
$$\times U_q^{l,m}(\omega', v_q) P_v(v_q) \mathrm{d}v_q \mathrm{d}\omega', \tag{14}$$

$$\langle |\Psi_{s,q}(\tau, v)|^2 \rangle = \frac{1}{\pi^2} \int_{-\infty}^{\infty} \int_{-\infty}^{\infty} \frac{S(\omega_1)}{k(\omega_1)} Q^*(\omega_1 - 2\pi v) \frac{S^*(\omega_2)}{k^*(\omega_2)}$$
$$\times Q(\omega_2 - 2\pi v) e^{-i(\omega_1 - \omega_2)\tau} \times \int \sum_l \sum_m \sum_n \sum_p$$
$$\times Q(\omega_1(1 + v_q(1/v_l^G + 1/v_m^G))^{-1})$$
$$\times U_q^{l,m,n,p}(\omega_1, \omega_2, v_q)$$
$$\times Q^*(\omega_2(1 + v_q(1/v_n^G + 1/v_p^G))^{-1})$$
$$\times P_v(v_q) \mathrm{d}v_q \mathrm{d}\omega_1 \mathrm{d}\omega_2, \tag{15}$$

where ω', ω_1 or ω_2 correspond to received frequencies,[14] v_m^G is the group velocity of the mth mode, and $Q(f)$is the source spectrum. As in the free-space case, the ambiguity function can also be interpreted in terms of target velocity and position by using the transformations $v = v_1^G v/(2f_c)$ and $u = v_1^G \tau/2$, where v and u are the target's velocity and position, and f_c is the signal's center frequency. The variables $U_q^{l,m}$ and $U_q^{l,m,n,p}$ are defined in Eqs. (B34) and (B38), respectively, and are characteristic functions for the qth target's initial position u_q^0 given its probability density function, $P_{\mathrm{u}}(\mathrm{u}_q^0)$. They can be interpreted as Fourier transforms of the target's spatial distribution and are evaluated at the Doppler-shifted frequencies $\omega_{m,l,q}$ and $\omega_{p,n,q}$ so that they are functions of the modes l, m, n, and p.

For a group containing N targets, we again have $|\langle \Psi_s(\tau, v) \rangle|^2 = N^2 |\langle \Psi_{\mathrm{s,q}}(\tau, v) \rangle|^2$ and $\langle |\Psi_s(\tau, v)|^2 \rangle = N \langle |\Psi_{\mathrm{s,q}}(\tau, v)|^2 \rangle + N(N-1) |\langle \Psi_{s,q}(\tau, v) \rangle|^2$. As in the free-space case, the expected square magnitude of the ambiguity function is the sum of a second moment term proportional to N and a mean-squared term proportional to N^2,where the variance term typically dominates for groups large compared to the wavelength,[6] as shown for the case A target distribution scenario that represents migrating herring (Table I) in Fig. 4. The source signal and remote sensing system parameters are given in Table II. We note that the targets appear to be closer to the source/receiver by roughly 40 m, but this is approximately equal to the length scale of the system's resolution footprint, so for practical purposes the targets are still accurately localized.

1. Estimating target position and velocity statistics

As in the free-space case, Eqs. (14) and (15) cannot typically be analytically evaluated. A significant simplification is however possible in the case of some specially designed source spectra, such as Costas sequences, which can be written in the form of Eq. (7), $Q(\Omega) = \sum_{n=0}^{M-1} a_n e^{i(\Omega - \Omega_n)H_n} \delta(\Omega - \Omega_n)$. The second moment of the ambiguity function is then given by (see Appendix B2),

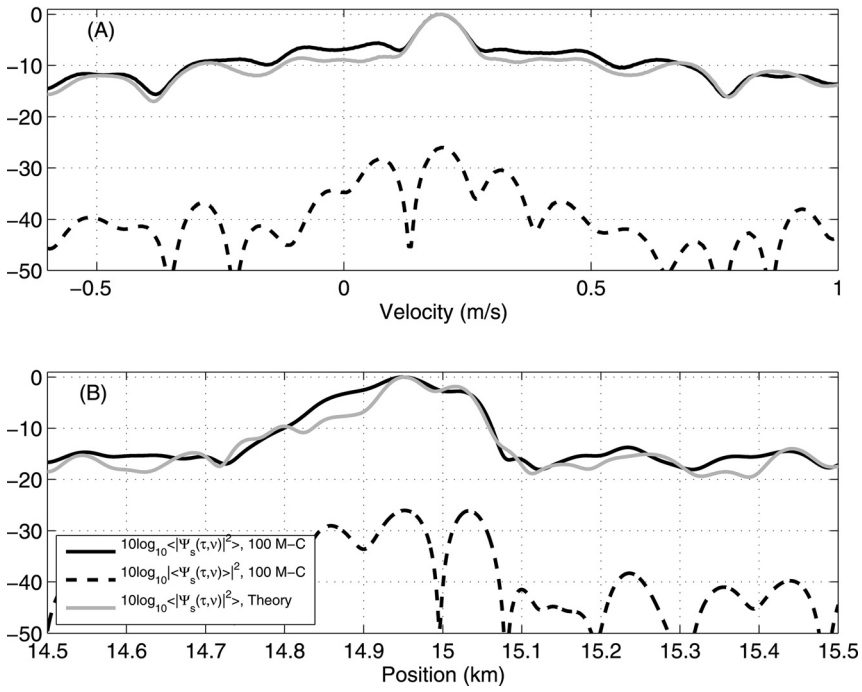

FIG. 4. Waveguide. $10\log_{10}\ \langle|\Psi(\tau,v)|\rangle^2$(black dashed line) and $10\log_{10}\ \langle|\Psi(\tau,v)|^2\rangle$ (black solid line) via 100 Monte-Carlo simulations for the field scattered from a random aggregation of targets following the case A scenario described in Table I. The cross-range resolution is set to be such that the fish areal number density is 2 fish/m^2. The source signal and remote sensing system parameters are given in Table II. $10\log_{10}$ of the expected square magnitude of the ambiguity function, based on evaluating Eqs. (14–15) and (6) is also shown (gray line) and is found to be in good agreement with the Monte-Carlo result. The variance of the ambiguity function dominates the total intensity and the magnitude squared of the ambiguity function's expected value is negligible.

$$\left\langle|\Psi_{s,q}(\tau,v)|^2\right\rangle = \sum_{n'}^{M-1}\sum_{m'}^{M-1}\sum_{l'}^{M-1}\sum_{j'}^{M-1}\frac{a^*_{n'}a_{m'}a_{l'}a^*_{j'}}{\pi^2} \times\left[\frac{S(\omega_{n'}+2\pi v)}{(\omega_{n'}+2\pi v)/c}\right]\left[\frac{S^*(\omega_{l'}+2\pi v)}{(\omega_{l'}+2\pi v)/c}\right] \times\delta\left(\frac{\omega_{j'}}{\omega_{m'}}-\frac{\omega_{l'}+2\pi v}{\omega_{n'}+2\pi v}\right)e^{-i(\omega_{n'}-\omega_{l'})\tau} \times\sum_{l}\sum_{m}\sum_{n}\sum_{p} \times U_q^{l,m,n,p}(\omega_{n'}+2\pi v,\omega_{l'}+2\pi v,\tilde{v}_q)P_v(\tilde{v}_q), \quad (16)$$

where $a_{n'}$ are the coefficients of the $\omega_{n'}$ frequency components for $n'=1,2,\ldots,M$, and

$$\tilde{v}_q=\left(\frac{\omega_{n'}+2\pi v}{\omega_{m'}}-1\right)(1/v_l^G+1/v_m^G)^{-1}. \quad (17)$$

Despite this simplified form, it is still not straightforward to derive analytical expressions for the moments along time-delay τ and Doppler shift v. We note, however, that

$$U_q^{l,m,n,p}(\omega_{n'}+2\pi v,\omega_{l'}+2\pi v,\tilde{v}_q) \equiv\frac{1}{V}\int_V\Phi^{l,m}_{s,q}(\mathrm{r},\omega_{m'},\omega_{n'}+2\pi v)\Phi^{*\,n,p}_{s,q}(\mathrm{r},\omega_{j'},\omega_{l'}+2\pi v)\mathrm{d}^3\mathrm{u}^0_q, \quad (18)$$

which is not a function of target velocity, so that Eq. (16) for the waveguide has many similarities with Eq. (8) for the free-space case. In the illustrative examples of Sec. III B, we assume the form of Eq. (9) still holds and use the coefficients of Table III for free-space to estimate the velocity means and standard deviations in a waveguide.

III. ILLUSTRATIVE EXAMPLES

Here, we demonstrate how the position and velocity mean and standard deviation of a group of targets can be simultaneously estimated in free-space and in a typical continental-shelf environment. We examine the three target scenarios described in Table I, which are illustrative of long-range remote sensing of marine life in the ocean. In all the examples, we employ the Costas sequence design detailed in Appendix A and the remote sensing system parameters summarized in Table II. The mean of the ambiguity function and its expected square magnitude are found by evaluating either Eqs. (4) and (5) for free-space or Eqs. (14) and (15) for the waveguide scenario via 100 Monte-Carlo simulations. We then evaluate the moments of the ambiguity function square magnitude along constant time-delay and Doppler shift axes. Estimates of the targets' velocity and position mean and standard deviation are obtained via the Moment Method by inverting Eqs. (9) and (11), using coefficients from Table III,

$$\hat{\mu}_{v,j}=\frac{v_1-c_1}{d_1}, \quad (19a)$$

$$\hat{\sigma}_{v,j}=\sqrt{\frac{v_2-c_2-d_2\hat{\mu}_{v,j}-e_2\hat{\mu}^2_{v,j}}{e_2}}, \quad (19b)$$

$$\hat{\mathrm{i}}_r\cdot\hat{\mu}_{\mathrm{u}}=\frac{c\tau_1}{d_3}-r, \quad (19c)$$

$$\hat{\mathrm{i}}_r\cdot\sigma_{\mathrm{u}}=\sqrt{\frac{c^2\tau_2}{2d_3}-[r+\hat{\mathrm{i}}_r\cdot\mu_{\mathrm{u}}]^2} \quad (19d)$$

where

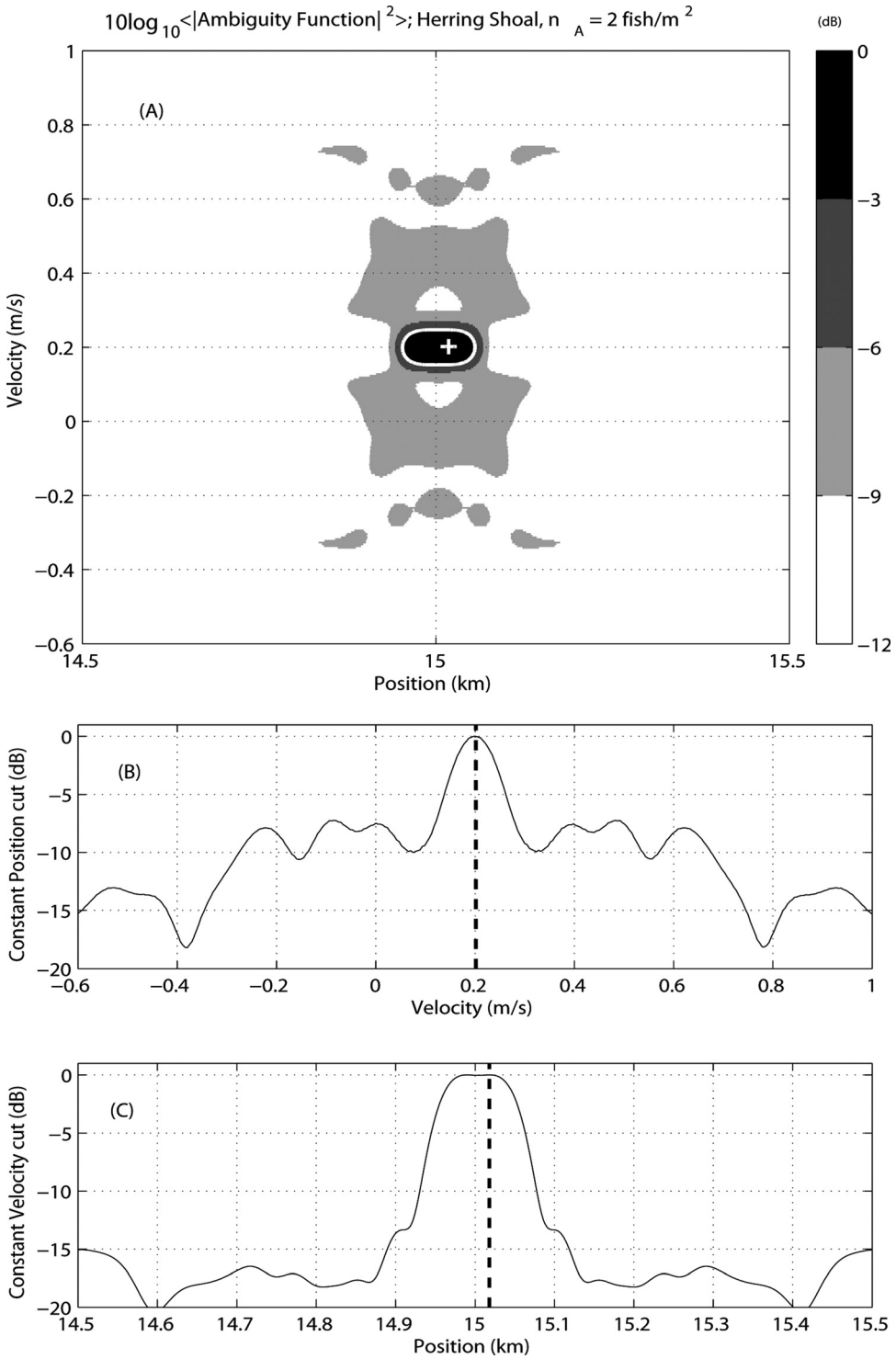

FIG. 5. Free-space. The strength of the sidelobes is much less than half that of the main lobe and the Moment Method provides accurate velocity and position estimates, as shown in Fig. 6. (A) $10\log_{10}$ of the expected value of the ambiguity function square magnitude for the pressure field scattered from a shoal of migrating herring (Table I, case A) and given the source signal and remote sensing system parameters in Table II. The white curve indicates 3 dB-down contour(s), which may be used to roughly delimit the target shoal. The maximum of the ambiguity surface is shown by a white cross. (B, C) Constant-velocity and constant-position cuts through the point indicated by the white cross in (A). Dashed lines indicate the mean position and velocity estimates based on the maximum value of the ambiguity surface (Peak Method).

$$d_3 = \sum_{n=0}^{M-1}\sum_{m=0}^{M-1} d_{n,m}, \tag{20}$$

$d_{n,m}$ has been defined in Eq. (12) and j corresponds to one Monte-Carlo simulation. For the coefficients c_1 through e_2, we use the analytically calculated values for free-space given in the first row of Table III. Estimates of the mean velocity and position are also obtained by simply finding the peak of the ambiguity function square magnitude, which we refer to as the Peak Method and define by

$$\langle|\Psi_{s,q}(\tau,v)|^2\rangle|_{v\,=\,2\hat{\mu}'_{v,j}f_c/c}, \tag{21a}$$

$$\langle|\Psi_{s,q}(\tau,v)|^2\rangle|_{\tau\,=\,2\hat{\mu}'_{u,j}/c}. \tag{21b}$$

For each estimated quantity, $N_{\mathrm{MC}} = 100$ Monte-Carlo simulations are used to calculate the estimate's sample mean and sample variance, and so investigate how such estimates perform in both free-space and waveguide environments. For example,

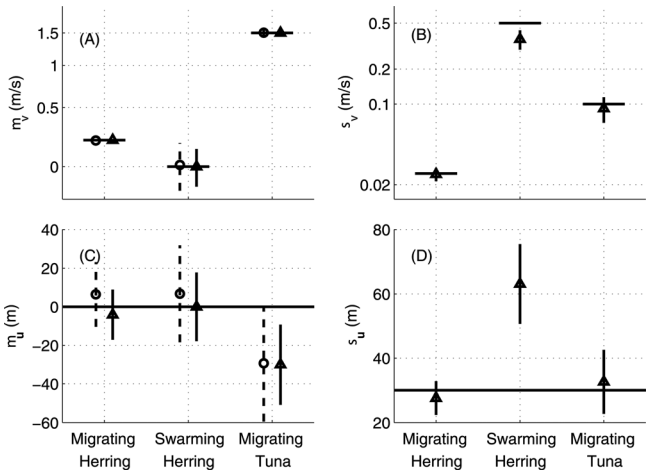

FIG. 6. Free-space. Estimates of the velocity and position mean and standard deviation for simulated migrating and swarming herring shoals, and a migrating school of tuna (Table I), given the source signal and remote sensing system parameters summarized in Table II. Target positions are localized within the remote sensing system's resolution footprint, and velocity estimate errors are typically less than roughly 10%. Horizontal lines indicate true values. (A, B) Estimates of the targets' velocity mean and standard deviation. Triangles and solid vertical lines indicate the sample means and sample standard deviations of estimates obtained via the Moment Method [Eqs. (19a) and (19b)], using 100 Monte-Carlo simulations. Circles and dashed lines indicate the sample mean and sample standard deviation for estimates of the mean velocity obtained via the Peak Method [Eq. (21a)], i.e., by locating the maximum of the ambiguity function square magnitude [white cross in Fig. 5(a)]. (C, D) Same as (A,B) but for estimates of the group's position mean and standard deviations obtained via both the moment (triangles and solid vertical lines) and peak (circles and dashed lines) methods.

$$\langle \hat{\mu}_v \rangle = \frac{1}{N_{MC}} \sum_{j=1}^{N_{MC}} \hat{\mu}_{v,j}, \tag{22a}$$

$$\mathrm{var}(\hat{\mu}_v) = \frac{1}{N_{MC}} \sum_{j=1}^{N_{MC}} (\hat{\mu}_{v,j} - \langle \hat{\mu}_v \rangle)^2 . \tag{22b}$$

The free-space results are presented here for comparison with those in a waveguide, since analytical expressions for the moments of the expected square magnitude of the ambiguity function have been derived only for free-space. For the waveguide scenarios, we check whether estimates of the velocity and position mean and standard deviation can be obtained via the Moment Method using the analytical expressions derived in free-space, Eqs. (9) and (11), and Table III. For the case when additive noise in included, the results presented here are applicable as long as the spectral level of the noise does not exceed the spectral level of the signal by more than the time-bandwidth product of the signal.

A. Free-space

The expected square magnitude of the ambiguity function, as well as constant-velocity and constant-position cuts through its maximum for a typical migrating shoal of herring (Table I, case A) are shown in Fig. 5, given the signal and remote sensing system parameters summarized in Table II. Estimates of the velocity and position mean are obtained via the Moment Method [Eqs. (19a) and (19c)], as well as via

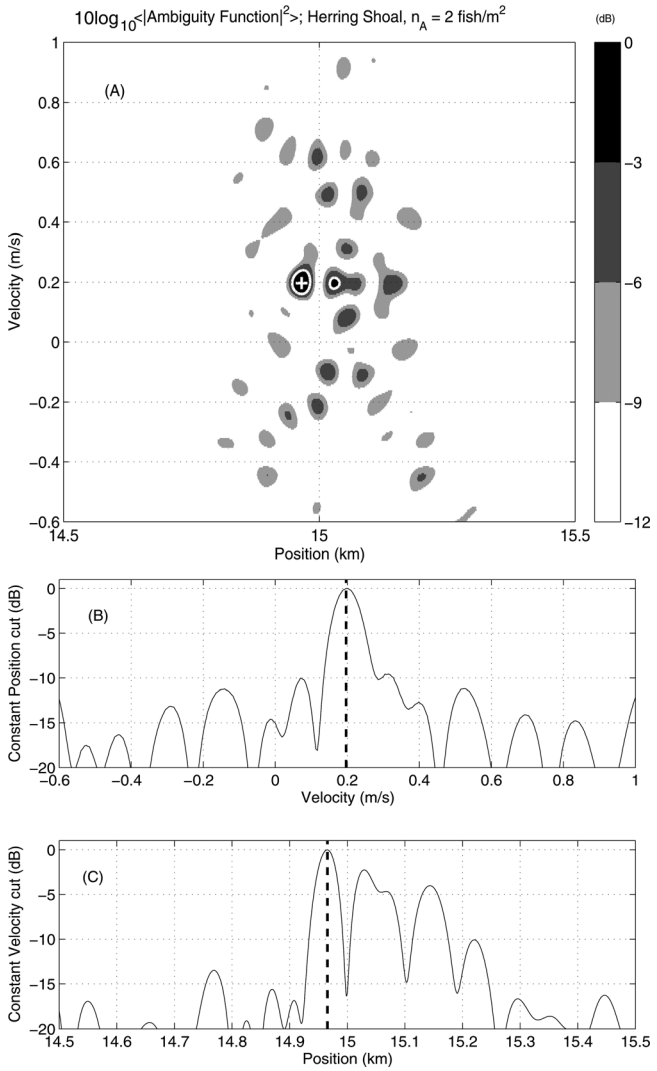

FIG. 7. Waveguide. There is now more energy in the sidelobes of the ambiguity function compared to Fig. 5, but both the Peak and Moment methods still provide accurate velocity and position estimates as seen in Fig. 8. (A) $10\log_{10}$ of the expected value of the ambiguity function square magnitude for the pressure field scattered from a shoal of migrating herring (Table I, case A) and given the source signal and remote sensing system parameters in Table II. The fish are assumed to be submerged in the waveguide of Fig. 2. The cross-range resolution is set to be such that the fish areal number density is 2 fish/m^2. The white curve indicated 3 dB-down contour(s), which may be used to roughly delimit the target shoal. The maximum of the ambiguity surface is shown by a white cross. (B, C) Constant-velocity and constant-position cuts through the point indicated by the white cross in (A). Dashed lines indicate the mean position and velocity estimates based on the maximum value of the ambiguity surface (Peak Method).

the Peak Method [Eq. (21)]. The Moment Method and Eqs. (19b) and (19d) are then used to estimate the velocity and position standard deviation.

The sample means and sample standard deviations, e.g., Eqs. (22a) and (22b), of these estimates are shown in Fig. 6. We find that estimates of the velocity and position mean based on the Moment Method are at least as accurate as those based on the Peak Method. For mean velocity, only the case of the swarming herring demonstrates an observable bias which is likely due to the very large standard deviation of the targets' velocity for that scenario. As long as the estimate of mean position is within the 40 m resolution footprint

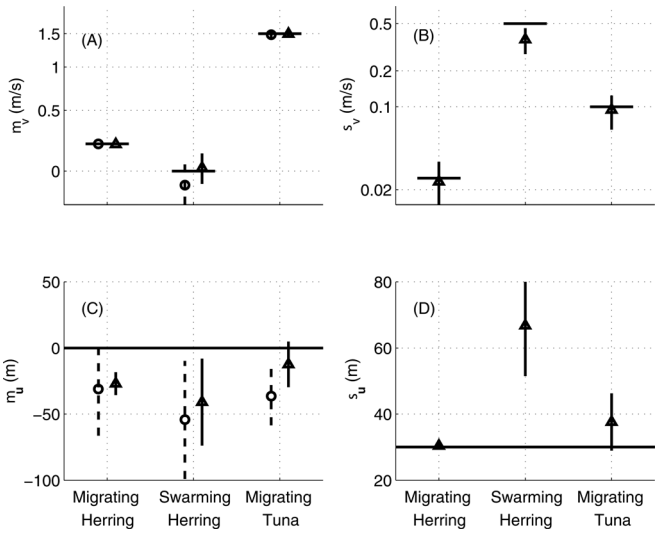

FIG. 8. Waveguide. Estimates of the velocity and position mean and standard deviation for simulated migrating and swarming herring shoals and a migrating school of tuna (Table I), given the source signal and remote sensing system parameters summarized in Table II. Target positions are localized within the remote sensing system's resolution footprint, and velocity estimate errors are typically less than roughly 10%. Horizontal lines indicate true values. (A, B) The sample means and sample standard deviations of estimates of the targets' velocities mean and standard deviation obtained via the Moment Method [Eqs. (19a) and (19b), triangles and solid vertical lines]. Also the sample mean and sample standard deviation of the target mean velocity estimate obtained via the Peak Method [Eq. (21a), circles and dashed lines], i.e., by locating the maximum of the ambiguity function (white cross in Fig. 7). (C, D) Same as (A, B) but for estimates of the group's position mean and standard deviations obtained via both the moment (triangles and solid vertical lines) and peak (circles and dashed lines) methods.

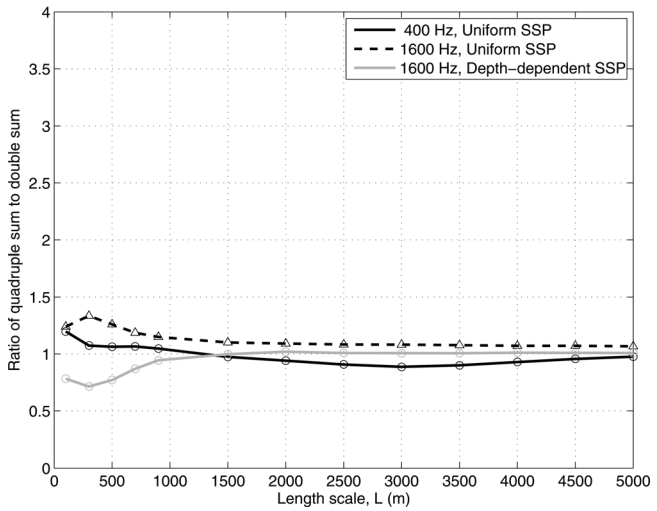

FIG. 9. Waveguide. Necessary length scales for the quadruple modal sum of Eq. (B37) to reduce to a double modal sum, given different frequencies Ω and sound speed profiles.

of the remote sensing system, for practical purposes, the target group has been accurately localized. This is the case for all the examples considered here, as shown in Fig. 6. Estimates of the velocity standard deviation for cases A, B, and C are very distinct. This suggests that in free-space it may be possible to use the Moment Method to help identify and classify dynamic behavior.

B. Waveguide

We consider the same cases (Table I) as in Sec. III A for free-space, with the same source signal and remote sensing system parameters (Table II), but now in the waveguide as shown in Fig. 2. For the case of a migrating herring shoal (Table I, case A), we find that the Peak and Moment Methods provide accurate velocity and position estimates, even though the ambiguity function square magnitude now exhibits more significant sidelobes, as shown in Fig. 7. By using Monte-Carlo simulations, we show that the same equations that linearly relate the first two moments of the ambiguity function square magnitude along a constant Doppler shift axis to the first two moments of the target swarm's position in free-space [Eqs. (11a and 11b)] also approximately hold in the waveguide case, for the Costas source signal.

These estimates for all cases are shown in Fig. 8. We find that the free-space expressions and coefficients for the Moment Method of Eqs. (9) and (11) and Table III provide very good estimates of the mean velocity and position of the groups and their standard deviation in a stratified range-independent waveguide environment. Estimates of the velocity mean and standard deviation are found to typically be within 10% of their true values, and the targets are accurately localized within the system's resolution footprint. Estimates of the velocity standard deviation for the three different cases considered are found to be distinct, which suggests that it may be possible to classify dynamic behavior through instantaneous Doppler measurements.

IV. CONCLUSIONS

We showed that for typical remote sensing scenarios of large aggregations of randomly distributed moving targets where the group dimensions are much larger than the acoustic wavelength, the variance of the scattered field dominates the range-velocity ambiguity function, but cross-spectral coherence remains and enables high resolution Doppler velocity and position estimation. We then developed a method for simultaneously and instantaneously estimating the means and standard deviations of the velocity and position of groups of self-propelled underwater targets from moments of the measured range-velocity ambiguity function. This Moment Method is based on analytic expressions for the expected square magnitude of the range-velocity ambiguity function *in free-space*. It was shown that for pseudo-random signals, such as Costas sequences, the moments of the ambiguity function's expected square magnitude along constant time-delay and Doppler shift are linear functions of the mean and variance of the targets' velocity and position. We also described an alternative Peak Method that can be used to estimate the targets' mean velocity and position.

Both methods were shown to perform well not only in free-space, but in a typical continental-shelf ocean waveguide also. In particular, for typical long-range imaging scenarios, exceeding 10 km, the target groups were accurately localized within the remote sensing system's resolution footprint with simultaneous velocity mean and standard deviation estimates for the group within 10% of the true values. We found that the estimates obtained via the Moment

Method were at least as accurate as those provided by the Peak Method. The performance of both methods is dependent on maintaining low sidelobes in the ambiguity surface. Since it is only possible to measure the targets' velocity component *relative* to the system, at least two sources or receivers must be used to estimate horizontal velocity vectors.

APPENDIX A: SIGNAL DESIGN

The range-velocity ambiguity function provides a graphical representation of the resolution capacity of a given signal and is typically used to quantify the signal's performance in terms of resolving target range and relative velocity from measurements of the scattered field.[1] The ambiguity function characteristics for several "basic" signals have been reviewed extensively in literature.[1,23–25] In terms of clutter discrimination and reverberation suppression in the presence of ambient noise, the following signals are among the best options: pulse trains, linear frequency modulated (LFM) signals, and pseudo-random noise signals, such as Costas sequences. Here, we describe the design of a Costas sequence signal motivated by the need to resolve the position and velocity of a large group of underwater biological targets. We assume that the desired range resolution is around 50 m, while the velocity resolution should be better than 0.2 m/s. Finally, the signal's center frequency should be on the order of hundreds of hertzs or a few kilohertz, to allow for remote sensing on the order of tens of kilometers.[20]

A Costas sequence is defined in terms of the number M of CW pulses in the sequence, the duration T_{cw} of each pulse, the base frequency f_b, and the sequence used to generate each CW pulse. To determine appropriate values for the above parameters, we consider the range $\Delta u = c\Delta\tau/2$ and velocity $\Delta v = c\Delta v/(2f_c)$resolutions we want to achieve, where $\Delta\tau$ and Δv are the time-delay and Doppler shift resolutions of the signal,[1]

$$\Delta\tau = \frac{1}{B} = \frac{T_{\mathrm{cw}}}{M}, \tag{A1a}$$

$$\Delta v = \frac{1}{T_{\mathrm{tot}}} = \frac{1}{MT_{\mathrm{cw}}}, \tag{A1b}$$

$f_c \equiv f_b + B/2$ is the center frequency and c is the speed of sound in the medium. Increasing the center frequency will decrease Δv and so increase the velocity resolution. Given then a Costas sequence of $M = 7$ pulses, a pulse length of $T_{\mathrm{cw}} = 0.4$ s leads to a range resolution of approximately 43 m in water ($c = 1500$ m/s). The desired velocity resolution of 0.2 m/s or better can then be achieved by choosing $f_c = 1600$ Hz to get $\Delta v \approx 0.17$ m/s.

For this specific design of a 7-pulse Costas sequence, the total signal duration is $T_{\mathrm{tot}} = MT_{\mathrm{cw}} = 2.8$ s and the bandwidth is $B = M/T_{\mathrm{cw}} \approx 20$ Hz. Each of the seven consequent pulses is a CW at frequency $f_n = f_b + \alpha_n/T_{\mathrm{cw}}$ for $n = 0,1,\ldots, M-1$, where f_b is the signal "base" frequency ($f_c - B/2$) and α_n is the $(n+1)$th element of the Costas sequence, here chosen to be (4, 7, 1, 6, 5, 2, 3). The normalized time domain expression is given by[1]

$$q(t) = \frac{1}{\sqrt{MT_{\mathrm{cw}}}} \sum_{n=0}^{M-1} q_n(t - nT_{\mathrm{cw}}) , \tag{A2}$$

where

$$q_n(t) = \begin{cases} e^{-i2\pi f_n t}, & 0 \le t \le T_{\mathrm{cw}} \\ 0, & \text{otherwise.} \end{cases} \tag{A3}$$

The complex signal spectrum is then given by the Fourier transform of Eq. (A2),

$$\begin{aligned} Q(f) &= \sqrt{\frac{T_{\mathrm{cw}}}{M}} \sum_{n=0}^{M-1} e^{i2\pi f(nT_{\mathrm{cw}})} e^{i2\pi(f-f_n)T_{\mathrm{cw}}/2} \sin c(\pi(f - f_n)T_{\mathrm{cw}}) \\ &= \sum_{n=0}^{M-1} a_n e^{i2\pi(f-f_n)h_n} \sin c(\pi(f - f_n)T_{\mathrm{cw}}) \\ &\approx \sum_{n=0}^{M-1} a_n e^{i2\pi(f-f_n)h_n} \delta(f - f_n), \end{aligned} \tag{A4}$$

where $a_n = \sqrt{\frac{T_{\mathrm{cw}}}{M}} e^{i2\pi f_n nT_{\mathrm{cw}}}$ and $h_n = (n + 1/2)T_{\mathrm{cw}}$, so that Eq. (A4) is in the form of Eq. (7). Note that the last line of Eq. (A4) strictly requires $|f - f_n| > 1/T_{\mathrm{cw}}$. It is still approximately valid otherwise.

APPENDIX B: FULL FORMULATIONS IN FREE-SPACE AND IN A STRATIFIED WAVEGUIDE FOR THE STATISTICAL MOMENTS OF THE AMBIGUITY FUNCTION FOR THE FIELD SCATTERED FROM A GROUP OF RANDOMLY DISTRIBUTED, RANDOMLY MOVING TARGETS

1. Free-space

Here, we derive analytical expressions for the statistical moments of the ambiguity function of the total acoustic field scattered from a group of moving targets in free-space. We begin with an analytical expression for the acoustic field scattered from a simple harmonic source by a single moving target in free-space (Appendix C of Ref. 14) and derive expressions for the statistical moments of the received field when the target's position and velocity are random. Fourier synthesis is then used to expand these expressions for the general case of broadband source signals and calculate the statistical moments of the ambiguity function of the received field. Accounting for the cumulative effect of a distribution of N randomly swarming targets, we note that the expected intensity of the received field consists of (i) a variance term proportional to N due to scattering from each target, and (ii) a mean-squared term proportional to N^2 due to interaction of the fields scattered from different targets,[22] where the variance term typically dominates.[6]

a. The back-scattered field

We consider a monostatic stationary source/receiver system at r, and a group of N targets randomly distributed in volume V centered at the origin 0. The random position of

the qth target at time t_q is given by $\mathrm{r}_q = \mathrm{u}_q^0 + \mathrm{v}_q t_q$, as shown in Fig. 1, where u_q^0 is its random initial position, and v_q is the target's average velocity during the time necessary for the sound signal to travel through the remote system's resolution footprint. Since the Doppler shift due to a moving target depends only on its speed relative to the source and receiver, we assume without loss of generality that $\mathrm{v}_q = v_q \hat{\mathrm{i}}_r + v_{q,\perp} \hat{\mathrm{i}}_{r,\perp}$, where $\hat{\mathrm{i}}_{r,\perp}$ denotes a unit vector perpendicular to $\hat{\mathrm{i}}_r$. Under the above conditions, the field incident on the qth target in the far-field of a harmonic source of frequency f is given by adapting Eq. (C3) of Ref. 14,

$$\Phi_{i,q}(r_q, t_q; f) = e^{i2\pi f(r - \hat{\mathrm{i}}_r \cdot \mathrm{u}_q^0 - v_q t_q)/c} e^{-2i\pi f t_q}, \tag{B1}$$

where $\mathrm{r} \equiv |\mathrm{r}|, \hat{\mathrm{i}}_r = \mathrm{r}/|r|$, and we have used the far-field approximation $|\mathrm{r}_q - \mathrm{r}| = r - \hat{\mathrm{i}}_r \cdot \mathrm{r}_q$, valid for $r \gg r_q$. To determine the field scattered from the qth target, we then follow the derivation procedure detailed in Eqs. (C4)–(C19) of Ref. 14,

$$\Phi_{s,q}(\mathrm{r}, t; f) = \frac{S(\bar{f})}{\bar{k}} G(0|\mathrm{r}, \bar{f}(1 + 2v_q/c)^{-1}) G(\mathrm{r}|0, \bar{f}) e^{-i2\pi \bar{f} t} \times e^{-i2\pi \bar{f}(1 + (1+2v_q/c)^{-1}) \hat{\mathrm{i}}_r \cdot \mathrm{u}_q^0 / c,} \tag{B2}$$

where

$$\bar{f} = \frac{f(1 + v_q/c)}{1 - v_q/c}, \text{or } \bar{f} \approx f(1 + 2v_q/c) \tag{B3}$$

is the Doppler-shifted frequency of the scattered field. This derivation is also consistent with the approach of Dowling and Williams,[26] Eqs. (9.1)–(9.7), for calculating the sound field due to a moving point source.

Let us now consider the effect of random target position and speed. Taking expectations over the random initial offset u_q^0, we define

$$U_q(\bar{f} \hat{\mathrm{i}}_r / c, v_q) \equiv p_{\mathrm{u}} \left(\frac{\bar{f} \hat{\mathrm{i}}_r}{c} \left[1 + \frac{1}{1 + 2v_q/c} \right] \right) = \int_V e^{-i2\pi \bar{f}(1 + (1+2v_q/c)^{-1}) \hat{\mathrm{i}}_r \cdot \mathrm{u}_q^0 / c} P_{\mathrm{u}}(\mathrm{u}_q^0) \mathrm{d}^3 \mathrm{u}_q^0, \tag{B4}$$

where $P_{\mathrm{u}}(\mathrm{u}_q^0)$ is the probability that the target initial position is u_q^0, and p_{u} is the corresponding characteristic function, i.e., the Fourier transform of P_{u}. Then,

$$\langle \Phi_{s,q}(\mathrm{r}, t; f) \rangle = \int \frac{S(\bar{f})}{\bar{k}} G(0|\mathrm{r}, \bar{f}(1 + 2v_q/c)^{-1} G(\mathrm{r}|0, \bar{f}) e^{-i2\pi \bar{f} t}, \times U_q(\bar{f} \hat{\mathrm{i}}_r / c, v_q) P_v(v_q) \mathrm{d}v_q \tag{B5}$$

where $P_v(v_q)$ is the probability that the target speed is v_q. We note that when the source frequency f becomes such that the wavelength c/f is much smaller than the length scale of the targets' spatial distribution, the variable $U_q(\bar{f} \hat{\mathrm{i}}_r / c, v_q)$ approaches zero, so that $\langle \Phi_{s,q}(\mathrm{r}, t; f) \rangle \approx 0$ also.

Finally, we can derive an expression for the autocorrelation of the scattered field from the qth target,

$$\begin{aligned} &\langle \Phi_{s,q}(\mathrm{r}, t; f) \Phi_{s,q}^*(\mathrm{r}, t + \tau; f) \rangle \\ &= \int \frac{S(\bar{f}) S^*(\bar{f})}{\bar{k}\bar{k}^*} G(\mathrm{r}|0, \bar{f}) e^{-i2\pi \bar{f} t} G^*(\mathrm{r}|0, \bar{f}) e^{i2\pi \bar{f}(t+\tau)} \\ &\times \int G(0|\mathrm{r}, \bar{f}(1 + 2v_q/c)^{-1}) e^{-i2\pi \bar{f} \hat{\mathrm{i}}_r \cdot \mathrm{u}_q^0 / c (1 + (1+2v_q/c)^{-1})} \\ &\times G^*(0|\mathrm{r}, \bar{f}(1 + 2v_q/c)^{-1}) e^{i2\pi \bar{f} \hat{\mathrm{i}}_r \cdot \mathrm{u}_q^0 / c (1 + (1+2v_q/c)^{-1})} \\ &\times P_u(\mathrm{u}_q^0) P_v(v_q) \mathrm{d}^3 \mathrm{u}_q^0 \mathrm{d}v_q \\ &= \int \frac{|S(\bar{f})|^2}{|\bar{k}|^2} |G(\mathrm{r}|0, \bar{f})|^2 |G(0|\mathrm{r}, \bar{f}(1 + 2v_q/c)^{-1})|^2 \\ &\times e^{i2\pi \bar{f} \tau} P_v(v_q) \mathrm{d}v_q. \end{aligned} \tag{B6}$$

b. Statistical moments of the ambiguity function

For a broadband source with source function $q(t) \iff Q(f)$, the scattered field is found by Fourier synthesis as

$$\Psi_{s,q}(\mathrm{r}, t) = \int \mathrm{d}f Q(f) \Phi_{s,q}(\mathrm{r}, t; f) \, . \tag{B7}$$

The ambiguity function of $\Psi_{s,q}(\mathrm{r}, t)$ is defined as

$$\begin{aligned} \Psi_{s,q}(\tau, v) &= \int_{-\infty}^{\infty} \Psi_{s,q}(\mathrm{r}, t) q^*(t - \tau) e^{i2\pi v t} \mathrm{d}t \\ &= \int_{-\infty}^{\infty} \Psi_{s,q}(\mathrm{r}, f') Q^*(f' - v) e^{-i2\pi (f' - v)\tau} \mathrm{d}f', \end{aligned} \tag{B8}$$

where * signifies complex conjugate and

$$\begin{aligned} \Psi_{s,q}(\mathrm{r}, f') &= \int \mathrm{d}t e^{i2\pi f' t} \int \mathrm{d}f Q(f) \Phi_{s,q}(\mathrm{r}, t; f) \\ &= \int \mathrm{d}t e^{i2\pi f' t} \int \mathrm{d}f Q(f) \frac{S(\bar{f})}{\bar{k}} G(0|\mathrm{r}, \bar{f}(1 + 2v_q/c)^{-1}) \\ &\times G(\mathrm{r}|0, \bar{f}) \times e^{-i2\pi \bar{f} t} e^{-i2\pi \bar{f}(1 + (1+2v_q/c)^{-1}) \hat{\mathrm{i}}_r \cdot \mathrm{u}_q^0 / c}. \end{aligned} \tag{B9}$$

Changing the order of integration, the integral over t results in the delta function $\delta(f' - \bar{f})$, where $f' = f(1 + 2v_q/c)$ (see Appendix B1). Substituting for f,

$$\begin{aligned} \Psi_{s,q}(\mathrm{r}, f') &= \int \frac{\delta(f' - \bar{f}) \mathrm{d}\bar{f}}{1 + 2v_q/c} Q(\bar{f}(1 + 2v_q/c)^{-1}) \\ &\times \frac{S(\bar{f})}{\bar{k}} G(0|\mathrm{r}, \bar{f}(1 + 2v_q/c)^{-1}) G(\mathrm{r}|0, \bar{f}) \\ &\times e^{-i2\pi \bar{f}(1 + (1+2v_q/c)^{-1}) \hat{\mathrm{i}}_r \cdot \mathrm{u}_q^0 / c} \\ &\approx \frac{S(f')}{k'} G(0|\mathrm{r}, f'(1 + 2v_q/c)^{-1}) G(\mathrm{r}|0, f') \\ &\times Q(f'(1 + 2v_q/c)^{-1}) \\ &\times e^{-i2\pi f'(1 + (1+2v_q/c)^{-1}) \hat{\mathrm{i}}_r \cdot \mathrm{u}_q^0 / c}. \end{aligned} \tag{B10}$$

Plugging Eq. (B10) into Eq. (B8), we then have

$$\Psi_{s,q}(\tau,v)=\int_{-\infty}^{\infty}\frac{S(f')}{k'}G(0|\mathrm{r},f'(1+2v_q/c)^{-1})\times G(\mathrm{r}|0,f')Q(f'(1+2v_q/c)^{-1})\times e^{-i2\pi f'(1+(1+2v_q/c)^{-1})\hat{\mathrm{i}}_r\cdot\mathrm{u}_q^0/c}\times Q^*(f'-v)e^{-i2\pi(f'-v)\tau}\mathrm{d}f' \quad \text{(B11)}$$

and we can now provide expressions for the expected value of the ambiguity function, as well as its second moment,

$$\langle\Psi_{s,q}(\tau,v)\rangle=\int_{-\infty}^{\infty}\frac{S(f')}{k'}G(\mathrm{r}|0,f')Q^*(f'-v)e^{-i2\pi(f'-v)\tau}\times\int G(0|\mathrm{r},f'(1+2v_q/c)^{-1})Q(f'(1+2v_q/c)^{-1})\times U_q(f'\hat{\mathrm{i}}_r/c,v_q)P_v(v_q)\mathrm{d}v_q\mathrm{d}f' \quad \text{(B12)}$$

and

$$\langle|\Psi_{s,q}(\tau,v)|^2\rangle=\int_{-\infty}^{\infty}\int_{-\infty}^{\infty}\frac{S(f_1)}{k_1}G(\mathrm{r}|0,f_1)Q^*(f_1-v)\times\frac{S^*(f_2)}{k_2^*}G^*(\mathrm{r}|0,f_2)Q(f_2-v)\times e^{-i2\pi(f_1-f_2)\tau}\times\int G(0|\mathrm{r},f_1(1+2v_q/c)^{-1})Q(f_1(1+2v_q/c)^{-1})\times G^*(0|\mathrm{r},f_2(1+2v_q/c)^{-1})Q^*(f_2(1+2v_q/c)^{-1})\times U_q((f_1-f_2)\hat{\mathrm{i}}_r/c,v_q)P_v(v_q)\mathrm{d}v_q\mathrm{d}f_1\mathrm{d}f_2. \quad \text{(B13)}$$

We note that the term U_q, which corresponds to the characteristic function of the random target position u_q^0, is evaluated at different wavenumbers between Eqs. (B12) and (B13). As demonstrated in Sec. II A, evaluating U_q near base-band typically leads to the second moment of the ambiguity function dominating over the magnitude squared of its first moment.

For the total field scattered from the group of N targets within volume V, we can write $\Psi_s(\mathrm{r},f')=\sum_{q=1}^{N}\Psi_{s,q}(\mathrm{r},f')$. Assuming that: (i) target positions are i.i.d.random variables, and (ii) target speeds are also i.i.d., we then have $\langle\Psi_s(\tau,v)\rangle = N\langle\Psi_{s,q}(\tau,v)\rangle$ with the second moment given by

$$\begin{aligned}\langle|\Psi_{s,q}(\tau,v)|^2\rangle=&\sum_{q=1}^{N}\sum_{p=1}^{N}\int_{-\infty}^{\infty}\int_{-\infty}^{\infty}\frac{S(f_1)}{k_1}G(\mathrm{r}|0,f_1)Q^*(f_1-v)\times\frac{S^*(f_2)}{k_2^*}G^*(\mathrm{r}|0,f_2)Q(f_2-v)\\&\times\int\int\int\int G(0|\mathrm{r},f_1(1+2v_q/c)^{-1})\times Q(f_1(1+2v_q/c)^{-1})G^*(0|\mathrm{r},f_2(1+2v_q/c)^{-1})\\&\times Q^*(f_2(1+2v_p/c)^{-1})e^{-i2\pi f_1(1+(1+2v_q/c)^{-1})\hat{\mathrm{i}}_r\cdot\mathrm{u}_q^0/c}\times e^{i2\pi f_2(1+(1+2v_q/c)^{-1})\hat{\mathrm{i}}_r\cdot\mathrm{u}_p^0/c}\\&\times P_{\mathrm{u}}(\mathrm{u}_q^0)P_{\mathrm{u}}(\mathrm{u}_p^0)P_v(v_q)P_v(v_p)\mathrm{d}\mathrm{u}_q^0\mathrm{d}\mathrm{u}_p^0\mathrm{d}v_q\mathrm{d}v_p\times e^{-i2\pi(f_1-f_2)\tau}\mathrm{d}f_1\mathrm{d}f_2\\=&N\langle|\Psi_{s,q}(\tau,v)|^2\rangle+N(N-1)|\langle\Psi_{s,q}(\tau,v)\rangle|^2.\end{aligned} \quad \text{(B14)}$$

The last line is arrived at by considering the distinction between the $q=p$ terms, and the $q\neq p$ terms. The second moment of the ambiguity function then consists of two terms: (i) a variance term proportional to N due to scattering from each target and (ii) a mean-squared term proportional to N^2 due to interaction of the fields scattered from different targets,[22] where the variance term typically dominates.[6]

c. Moments of the ambiguity function over time delay and Doppler shift

Equations (B12) and (B13) cannot typically be analytically evaluated. A significant simplification is however possible in the case of specially designed source spectra that can be approximated by Eq. (7), $Q(f)=\sum_{n=0}^{M-1}a_n e^{i2\pi(f-f_n)h_n}\delta(f-f_n)$. As we show in Appendix A, a Costas sequence belongs in this set of signals. Equation (B12) can then be rewritten as,

$$\begin{aligned}\langle\Psi_{s,q}(\tau,v)\rangle=&\sum_{n=0}^{M-1}\sum_{m=0}^{M-1}a_n^*a_m\int_{-\infty}^{\infty}\frac{S(f')}{k'}G(\mathrm{r}|0,f')\times e^{-i2\pi(f'-v-f_n)h_n}\delta(f-v-f_n)\\&\times e^{-i2\pi(f'-v)\tau}\int G(0|\mathrm{r},f'(1+2v_q/c)^{-1})\times e^{i2\pi(f'(1+2v_q/c)^{-1}-f_m)h_m}\times\delta(f'(1+2v_q/c)^{-1}\\&-f_m)U_q(f'\hat{\mathrm{i}}_r/c,v_q)P_v(v_q)\mathrm{d}v_q\mathrm{d}f'.\end{aligned} \quad \text{(B15)}$$

Integrating over f' introduces the delta function

$$\delta\left(v_q-\frac{c}{2}\left[\frac{f_n+v}{f_m}-1\right]\right), \quad \text{(B16)}$$

since $f'=f_n+v=f_m(1+2v_q/c)$, so that

$$\begin{aligned}\langle\Psi_{s,q}(\tau,v)\rangle=&\sum_{n=0}^{M-1}\sum_{m=0}^{M-1}a_n^*a_m\frac{S(f_n+v)}{2\pi(f_n+v)/c}G(\mathrm{r}|0,f_n+v)\\&\times G(0|\mathrm{r},f_m)e^{-i2\pi f_n\tau}\times p_{\mathrm{u}}([f_n+f_m+v]\hat{\mathrm{i}}_r/c)\\&\times P_v\left(\frac{c}{2}\left[\frac{f_n+v}{f_m}-1\right]\right),\end{aligned} \quad \text{(B17)}$$

where we have substituted for $U_{b,\mathrm{q}}$ using Eq. (B4). Similarly, for the second moment of the ambiguity function we find,

$$\begin{aligned}\langle|\Psi_{s,q}(\tau,v)|^2\rangle=&\sum_{n=0}^{M-1}\sum_{m=0}^{M-1}\sum_{l=0}^{M-1}\sum_{j=0}^{M-1}a_n^*a_ma_la_j^*\left[\frac{S(f_n+v)}{2\pi(f_n+v)/c}\right]\\&\times\left[\frac{S^*(f_l+v)}{2\pi(f_l+v)/c}\right]G(\mathrm{r}|0,f_n+v)\\&\times G^*(\mathrm{r}|0,f_l+v)G(0|\mathrm{r},f_m)G^*\left(0|\mathrm{r},\frac{f_l+v}{f_n+v}f_m\right)\\&\times\delta\left(\frac{f_l+v}{f_n+v}f_m-f_j\right)p_{\mathrm{u}}\left(\left[f_n+f_m-f_l-\frac{f_l+v}{f_n+v}f_m\right]\hat{\mathrm{i}}_r/c\right)\\&\times e^{-i2\pi(f_n-f_l)\tau}P_v\left(\frac{c}{2}\left[\frac{f_n+v}{f_m}-1\right]\right)\end{aligned} \quad \text{(B18)}$$

where the delta function signifies that, for given v, only specific frequency ratios result in non-zero values for $\langle|\Psi_{s,q}(\tau,v)|^2\rangle$.

To evaluate the moments of the ambiguity function's expected square magnitude along v, we assume that the acoustic wavelength is much smaller than the spatial extent of the target swarm, so that the characteristic function of the target's position (p_{u}) can be approximated as a delta function, whereby

$$\sum_{l=0}^{M-1}\sum_{j=0}^{M-1}\delta\left(\frac{f_l+v}{f_n+v}f_m-f_j\right)\delta\left(\left[f_n+f_m-f_l-\frac{f_l+v}{f_n+v}f_m\right]\right)\equiv\sum_{l=0}^{M-1}\sum_{j=0}^{M-1}\delta(f_l-f_n)\delta(f_j-f_m) \tag{B19}$$

so that

$$\langle|\Psi_{s,q}(\tau,v)|^2\rangle\sum_{n=0}^{M-1}\sum_{m=0}^{M-1}|a_n|^2|a_m|^2\frac{|S(f_n+v)|^2}{[2\pi(f_n+v)/c]^2}\times\frac{1}{4\pi r^4}P_v\left(\frac{c}{2}\left[\frac{f_n+v}{f_m}-1\right]\right). \tag{B20}$$

It has been shown in Ref. 22 that, for the opposite case, when the acoustic wavelength is on the order of the target swarm dimensions, other coherent effects are important and simplifications to Eq. (B18) are not possible. For low Mach number motions, we assume that the term $|S(f_n+v)|^2/[2\pi(f_n+v)/c]^2$ is approximately constant and equal to $|S(f_n)|^2/(2\pi f_n/c)^2$. The moments of Eq. (B20) along v for constant τ are linearly related to the moments of the target speed probability density,

$$v_1\equiv\int v\langle|\Psi_{s,q}(\tau,v)|^2\rangle\mathrm{d}v=\sum_{n,m}^{M-1}b_{n,m}\frac{2f_m}{c}\left(f_m-f_n+f_m\frac{2\mu_v}{c}\right), \tag{B21a}$$

$$v_2\equiv\int v^2\langle|\Psi_{s,q}(\tau,v)|^2\rangle\mathrm{d}v=\sum_{n,m}^{M-1}b_{n,m}\frac{2f_m}{c}\left\{\left(f_m-f_n+f_m\frac{2\mu_v}{c}\right)^2+\frac{4\sigma_v^2}{c^2}f_m^2\right\}, \tag{B21b}$$

after normalizing so that $\int\langle|\Psi_{s,q}(\tau,v)|^2\rangle\mathrm{d}v=1$, where $b_{n,m}$ is a known constant, μ_v and σ_v are the mean and standard deviation of the target speed, and f_n and f_m are known constants that correspond to the distinct frequency components of the source spectrum of Eq. (7). For example, for the case of a continuous harmonic wave ($M=1$), we find $v_1=2f_0\mu_v/c$, and $v_2=4f_0^2(\sigma_v^2+\mu_v^2)/c^2$.

Going back to Eq. (B18), to evaluate the moments of the ambiguity function's expected square magnitude along τ, we now write the characteristic function for u as a Taylor series expansion,

$$\begin{aligned}p_{\mathrm{u}}(\gamma\hat{\mathrm{i}}_r/c)&\equiv\int P_{\mathrm{u}}(\mathrm{u}_q)e^{-i2\pi\gamma\hat{\mathrm{i}}_r\cdot\mathrm{u}_q/c}\mathrm{d}\mathrm{u}_q=\int P_{\mathrm{u}}(\mathrm{u}_q)\Big(1-i2\pi\gamma\hat{\mathrm{i}}_r\cdot\mathrm{u}_q/c\\&\quad-\frac{4\pi^2}{2}[\gamma\hat{\mathrm{i}}_r\cdot\mathrm{u}_q/c]^2+\cdots\Big)\mathrm{d}\mathrm{u}_q\\&=1-i2\pi\gamma(r+\hat{\mathrm{i}}_r\cdot\mu_{\mathrm{u}})/c-\frac{4\pi^2}{2}\gamma^2([\hat{\mathrm{i}}_r\cdot\sigma_{\mathrm{u}}]^2\\&\quad+[r+\hat{\mathrm{i}}_r\cdot\mu_{\mathrm{u}}]^2)/c^2+\cdots=\sum_{d=0}^{p}c_d\gamma^d\end{aligned} \tag{B22}$$

where $\gamma=(f_n+f_m-f_l-f_m(f_l+v)/(f_n+v))$, and μ_{u} and σ_{u} are the mean and standard deviation of the target initial position, respectively. The moments of Eq. (B18) along τ involve integrals of the form

$$\int\tau^p e^{-i2\pi(f_n-f_l)\tau}\mathrm{d}\tau=\left(\frac{i}{2\pi}\right)^p\delta^{(p)}(f_n-f_l), \tag{B23}$$

where $\delta^{(p)}$ is the pth derivative of the Dirac delta function and is defined by the property j

$$\begin{aligned}\int h(f)\delta^{(p)}(f)\mathrm{d}f&=-\int\frac{\partial h(f)}{\partial f}\delta^{(p-1)}(f)\mathrm{d}f\\&=(-1)^p\int\frac{\partial^p h(f)}{\partial f^p}\delta(f)\mathrm{d}f.\end{aligned} \tag{B24}$$

Before substituting into Eq. (B18), we also note that

$$\sum_{l=0}^{M-1}\delta\left(\frac{f_l+v}{f_n+v}f_m-f_j\right)\delta(f_n-f_l)\equiv\delta(f_j-f_m)\ . \tag{B25}$$

The moments of Eq. (B18) along τ are then given by

$$\int\tau^p\langle|\Psi_{s,q}(\tau,v)|^2\rangle\mathrm{d}\tau=\sum_{n=0}^{M-1}\sum_{m=0}^{M-1}|a_n|^2|a_m|^2\frac{|S(f_n+v)|^2}{[2\pi(f_n+v)/c]^2}\frac{1}{(4\pi r)^4}\times p!\left(\frac{i}{2\pi}\right)^p c_p P_v\left(\frac{c}{2}\left[\frac{f_n+v}{f_m}-1\right]\right), \tag{B26}$$

so that

$$\tau_1\equiv\int\tau\langle|\Psi_{s,q}(\tau,v)|^2\rangle\mathrm{d}\tau=(r+\hat{\mathrm{i}}_r\cdot\mu_{\mathrm{u}})\frac{1}{c}\sum_{n=0}^{M-1}\sum_{m=0}^{M-1}P_v\left(\frac{c}{2}\left[\frac{f_n+v}{f_m}-1\right]\right), \tag{B27a}$$

$$\tau_2\equiv\int\tau^2\langle|\Psi_{s,q}(\tau,v)|^2\rangle\mathrm{d}\tau=\frac{2}{c^2}([\hat{\mathrm{i}}\cdot\sigma_{\mathrm{u}}]^2+[r+\hat{\mathrm{i}}_r\cdot\mu_{\mathrm{u}}]^2)\times\sum_{n=0}^{M-1}\sum_{m=0}^{M-1}P_v\left(\frac{c}{2}\left[\frac{f_n+v}{f_m}-1\right]\right). \tag{B27b}$$

Note here that, for the case of a continuous harmonic wave ($M=1$), it is not possible to infer the statistics of target position since $\gamma=0$, $p_{\mathrm{u}}(0)=1$, and the magnitude square of the ambiguity function does not depend on target position, as expected.

Also note that Eqs. (B21)–(B27) were derived for the expected value of the ambiguity function magnitude squared given a single target with random position and velocity, Eq. (B13). For a total of N targets, the expected value of the ambiguity function magnitude squared is instead given by Eq. (B14), which also involves the magnitude squared of the expected value of the ambiguity function for a single target, Eq. (B12). Moments of the latter along constant-τ and constant-v axis cannot in general be expressed as linear functions of the target's position and velocity statistical moments, even for source signals that satisfy Eq. (7). For a group of N targets, moments of the expected value of the total ambiguity function magnitude squared can still be used to obtain estimates of the targets' position and velocity means and standard deviations, as long as the variance of the received field intensity dominates, which is typically the case.[6]

2. Stratified waveguide

Here, we derive expressions for the statistical moments of the ambiguity function of the total acoustic field scattered from a group of moving targets in a stratified waveguide. Our formulation is based on analytical expressions for the Doppler shift and spread expected in long-range scattering from fish groups in the continental-shelf, which in turn are based on a model for scattering from a moving target submerged in a stratified ocean waveguide.[14] We also state conditions for modal decorrelation, since it has been shown that given a sufficiently large distribution of random volume or surface inhomogeneities, the waveguide modes will decouple in the mean forward field.[22,27]

a. The back-scattered field

As for the free-space case in Appendix B1, we consider a monostatic stationary system at range $\mathbf{r}$ from a group of N targets randomly distributed within volume V centered at the origin 0. The position of the qth target at time t_q is given by $\mathrm{r}_q = \mathrm{u_q}^0 + \mathrm{v}_q \mathrm{t}_q$, as shown in Fig. 1, where $\mathrm{u}^0{}_q$ is the initial random target position, and v_q is the target's average velocity during the time needed for the sound signal to travel through the remote system's resolution footprint. We assume again that $\mathrm{v}_q = v_q \hat{\mathrm{i}}_r + v_{q\perp} \hat{\mathrm{i}}_{r,\perp}$, where $\hat{\mathrm{i}}_{r,\perp}$ denotes a unit vector perpendicular to $\hat{\mathrm{i}}_r$. Finally, we assume that for the frequency regime we consider, the targets scatter omnidirectionally so that their scatter function has no angular dependence. Under the above conditions, we can rewrite Eq. (59) of Ref. 14 as

$$\Phi_{s,q}(r,t;\Omega) = 4\pi \sum_l \sum_m \frac{S(\omega_{m,l,q})}{k(\omega_{m,l,q})} \Phi^{l,m}_{s,q}(\mathrm{r},\Omega,\omega_{m,l,q}) e^{-i\omega_{m,l,q}t}, \tag{B28}$$

where

$$\omega_{m,l,q} = \Omega + v_q[\xi_l(\Omega) + \xi_m(\Omega)] \tag{B29}$$

is the Doppler-shifted frequency due to target motion. We have defined for convenience

$$\begin{aligned}\Phi^{l,m}_{s,q}(r,\Omega,\omega_{m,l,q}) = {} & [A_l(\mathrm{r};\Omega)A_m(\mathrm{r};\omega_{m,l,q})\mathrm{e}^{i(\gamma_l(\Omega)+\gamma_m(\omega_{m,l,q}))z^0_q} \\ & - A_l(\mathrm{r};\Omega)B_m(\mathrm{r};\omega_{m,l,q})\mathrm{e}^{i(\gamma_l(\Omega)-\gamma_m(\omega_{m,l,q}))z^0_q} \\ & - B_l(\mathrm{r};\Omega)A_m(\mathrm{r};\omega_{m,l,q})\mathrm{e}^{-i(\gamma_l(\Omega)-\gamma_m(\omega_{m,l,q}))z^0_q} \\ & + B_l(\mathrm{r};\Omega)B_m(\mathrm{r};\omega_{m,l,q})\mathrm{e}^{-i(\gamma_l(\Omega)+\gamma_m(\omega_{m,l,q}))z^0_q}] \\ & \times \mathrm{e}^{i(\xi_l(\Omega)+\xi_m(\omega_{m,l,q}))\rho^0_q}\end{aligned} \tag{B30}$$

where, other than in the expression for $\omega_{m,l,q}$, the lth mode wavenumbers are evaluated at Ω, while the mth mode wavenumbers are evaluated at $\omega_{m,l,q}$. Note that $\Phi^{l,m}_{s,q}(\mathrm{r},\Omega,\omega_{m,l,q})$ is an implicit function of v_q.

Equation (B28) is valid when we are in the far-field of the source/receiver, which is satisfied here since we are considering scattering from targets within a resolution footprint of our monostatic system. We have already made use of this fact in deriving Eq. (B30), where for the amplitudes of the down- and up-going plane waves of the incoming mode l, we have written

$$A_l(\mathrm{r}-\mathrm{u}^0_q;\Omega) = A_l(\mathrm{r};\Omega) \times e^{i(\xi_l(\Omega)\hat{\mathrm{i}}_\rho\cdot\mathrm{u}^0_q + \gamma_l(\Omega)\hat{\mathrm{i}}_z\cdot\mathrm{u}^0_q)}, \tag{B31a}$$

$$B_l(\mathrm{r}-\mathrm{u}^0_q;\Omega) = B_l(\mathrm{r};\Omega) \times e^{i(\xi_l(\Omega)\hat{\mathrm{i}}_\rho\cdot\mathrm{u}^0_q - \gamma_l(\Omega)\hat{\mathrm{i}}_z\cdot\mathrm{u}^0_q)}, \tag{B31b}$$

and similarly for the plane wave amplitudes of the outgoing mode m, we have used

$$\begin{aligned}A_m(\mathrm{r}-\mathrm{u}^0_q;\omega_{m,l,q}) = {} & A_m(\mathrm{r};\omega_{m,l,q}) \\ & \times e^{i(\xi_m(\omega_{m,l,q})\hat{\mathrm{i}}_\rho\cdot\mathrm{u}^0_q + \gamma_m(\omega_{m,l,q})\hat{\mathrm{i}}_z\cdot\mathrm{u}^0_q)},\end{aligned} \tag{B32a}$$

$$\begin{aligned}B_m(\mathrm{r}-\mathrm{u}^0_q;\omega_{m,l,q}) = {} & B_m(\mathrm{r};\omega_{m,l,q}) \\ & \times e^{i(\xi_m(\omega_{m,l,q})\hat{\mathrm{i}}_\rho\cdot\mathrm{u}^0_q - \gamma_m(\omega_{m,l,q})\hat{\mathrm{i}}_z\cdot\mathrm{u}^0_q)}.\end{aligned} \tag{B32b}$$

For spatial cylindrical coordinates $\mathrm{k} = \xi\hat{\mathrm{i}}_\rho + \gamma\hat{\mathrm{i}}_z$, while $A_l(r;\Omega)$, $B_l(r;\Omega)$ are the amplitudes of the down- and up-going modal plane wave components incident on the target, and $A_m(r;\omega_{m,l,q})$ and $B_m(\mathrm{r};\omega_{m,l,q})$are the amplitudes of the down- and up-going modal plane wave components scattered from the target,

$$A_l(\mathrm{r};\Omega) = \frac{i}{d(z)} \frac{e^{-i\pi/4} u_l(z) N^{(1)}_l}{\sqrt{8\pi\xi_l(\Omega)|\rho|}} e^{i(\xi_l(\Omega)|\rho| + \gamma_l(\Omega)z_t)}, \tag{B33a}$$

$$B_l(\mathrm{r};\Omega) = \frac{i}{d(z)} \frac{e^{-i\pi/4} u_l(z) N^{(2)}_l}{\sqrt{8\pi\xi_l(\Omega)|\rho|}} e^{i(\xi_l(\Omega)|\rho| - \gamma_l(\Omega)z_t)}, \tag{B33b}$$

$$A_m(\mathrm{r};\omega_{m,l,q}) = \frac{i}{d(0)} \frac{e^{-i\pi/4} u_m(z) N^{(1)}_m}{\sqrt{8\pi\xi_m(\omega_{m,l,q})|\rho|}} e^{i(\xi_m(\omega_{m,l,q})|\rho| + \gamma_m(\omega_{m,l,q})z_t)}, \tag{B33c}$$

$$B_m(\mathrm{r};\omega_{m,l,q}) = \frac{i}{d(0)} \frac{e^{-i\pi/4} u_m(z) N^{(2)}_m}{\sqrt{8\pi\xi_m(\omega_{m,l,q})|\rho|}} e^{i(\xi_m(\omega_{m,l,q})|\rho| - \gamma_m(\omega_{m,l,q})z_t)}. \tag{B33d}$$

Before taking expectations over target position and speed in Eq. (B28), we note that only $\Phi_{s,q}^{l,m}$ is a function of u_q^0 and define

$$U_q^{l,m}(\omega_{m,l,q}, v_q) \equiv \frac{1}{V}\int_V \Phi_{s,q}^{l,m}(\mathrm{r},\Omega,\omega_{m,l,q})\mathrm{d}^3\mathrm{u}_q^0$$
$$= \mathrm{sinc}((\xi_{lx}+\xi_{mx})L_x/2)\mathrm{sinc}((\xi_{ly}+\xi_{my})L_y/2)$$
$$\times [\mathrm{sinc}((\gamma_l+\gamma_m)L_z/2)(A_lA_m+B_lB_m),$$
$$-\mathrm{sinc}((\gamma_l-\gamma_m)L_z/2)(A_lB_m+B_lA_m)] \quad \text{(B34)}$$

where we have assumed that the target position is randomly distributed within the resolution footprint of volume V, and the following shorthand notations have been employed: $A_l = A_l(\mathrm{r};\Omega)$, $B_l = B_l(\mathrm{r};\Omega)$, $A_m = A_m(\mathrm{r};\omega_{m,l,q})$, and $B_m = B_m(\mathrm{r};\omega_{m,l,q})$. Note that ξ_{lx}, ξ_{ly}, and γ_l are evaluated at Ω, while ξ_{mx}, ξ_{my}, and γ_m are evaluated at $\omega_{m,l,q}$. We can then write for the expected value of field scattered from the qth target,

$$\langle\Phi_{s,q}(r,t;\Omega)\rangle = 4\pi\int\sum_l\sum_m \frac{S(\omega_{m,l,q})}{k(\omega_{m,l,q})}U_q^{l,m}(\omega_{m,l,q},v_q)$$
$$\times\, e^{-i\omega_{m,l,q}t}P_v(v_q)\mathrm{d}v_q, \quad \text{(B35)}$$

where $P_v(v_q)$ is the probability that the target speed is v_q. For small Mach numbers, the change between wavenumbers $\xi_l(\Omega)$ and $\xi_l(\omega_{m,l,q})$, as well as the change between modal amplitudes $A_l(\Omega)$ and $A_l(\omega_{m,l,q})$ are both very small, so that modal orthogonality leads to $\sum_l\sum_m U_q^{l,m}(\omega_{m,l,q},v_q) = \sum_l U_q^{l,l}(\omega_{l,l,q},v_q)$, where

$$U_q^{l,l}(\omega_{l,l,q}) = \mathrm{sinc}(\xi_{lx}L_x)\mathrm{sinc}(\xi_{ly}L_y)$$
$$\times [\mathrm{sinc}(\gamma_l L_z)(A_l^2+B_l^2) - 2A_lB_l]. \quad \text{(B36)}$$

When the length scale of the resolution footprint becomes sufficiently larger than the wavelength, the mean scattered field $\langle\Phi_{s,q}(\mathrm{r},t;\Omega)\rangle \approx 0$.

For the autocorrelation of the scattered field, we find

$$\langle\Phi_{s,q}(\mathrm{r},t;\Omega)\Phi_{s,q}^*(\mathrm{r},t+\tau;\Omega)\rangle$$
$$= \frac{16\pi^2}{V}\int\int_V\sum_l\sum_m\sum_n\sum_p \frac{S(\omega_{m,l,q})S^*(\omega_{p,n,q})}{k(\omega_{m,l,q})k^*(\omega_{p,n,q})}$$
$$\times \Phi_{s,q}^{l,m}(r,\Omega,\omega_{m,l,q})\Phi_{s,q}^{*n,p}(\mathrm{r},\Omega,\omega_{p,n,q})$$
$$\times e^{-iv_q[\xi_l(\Omega)+\xi_m(\Omega)-\xi_n(\Omega)-\xi_p(\Omega)]t}$$
$$\times e^{iv_q[\xi_n(\Omega)+\xi_p(\Omega)]\tau}e^{i\Omega\tau}P_v(v_q)\mathrm{d}^3\mathrm{u}_q^0\mathrm{d}v_q$$
$$= 16\pi^2\int\sum_l\sum_m\sum_n\sum_p \frac{S(\omega_{m,l,q})S^*(\omega_{p,n,q})}{k(\omega_{m,l,q})k^*(\omega_{p,n,q})}$$
$$\times U_q^{l,m,n,p}(\omega_{m,l,q},\omega_{p,n,q},v_q)e^{iv_q[\xi_n(\Omega)+\xi_p(\Omega)]\tau}e^{i\Omega\tau}$$
$$\times e^{-iv_q[\xi_l(\Omega)+\xi_m(\Omega)-\xi_n(\Omega)-\xi_p(\Omega)]t}P_v(v_q)\mathrm{d}v_q \quad \text{(B37)}$$

by defining

$$U_q^{l,m,n,p}(\omega_{m,l,q},\omega_{p,n,q},v_q)$$
$$\equiv \frac{1}{V}\int_V \Phi_{s,q}^{l,m}(\mathrm{r},\Omega,\omega_{m,l,q})\Phi_{s,q}^{*n,p}(\mathrm{r},\Omega,\omega_{p,n,q})\mathrm{d}^3\mathrm{u}_q^0$$
$$= \mathrm{sinc}((\xi_{lx}+\xi_{mx}-\xi_{nx}-\xi_{px})L_x/2)$$
$$\mathrm{sinc}((\xi_{ly}+\xi_{my}-\xi_{ny}-\xi_{py})L_y/2)$$
$$\times (A_lA_mA_n^*A_p^*+B_lB_mB_n^*B_p^*)[\mathrm{sinc}((\gamma_l+\gamma_m-\gamma_n-\gamma_p)L_z/2)$$
$$-(A_lA_mA_n^*B_p^*+B_lB_mB_n^*A_p^*)[\mathrm{sinc}((\gamma_l+\gamma_m-\gamma_n+\gamma_p)L_z/2)$$
$$-(A_lA_mB_n^*A_p^*+B_lB_mA_n^*B_p^*)[\mathrm{sinc}((\gamma_l+\gamma_m+\gamma_n-\gamma_p)L_z/2)$$
$$+(A_lA_mB_n^*B_p^*+B_lB_mA_n^*A_p^*)[\mathrm{sinc}((\gamma_l+\gamma_m+\gamma_n+\gamma_p)L_z/2)$$
$$-(A_lB_mA_n^*A_p^*+B_lA_mB_n^*B_p^*)[\mathrm{sinc}((\gamma_l-\gamma_m-\gamma_n-\gamma_p)L_z/2)$$
$$+(A_lB_mA_n^*B_p^*+B_lA_mB_n^*A_p^*)[\mathrm{sinc}((\gamma_l-\gamma_m-\gamma_n+\gamma_p)L_z/2)$$
$$+(A_lB_mB_n^*A_p^*+B_lA_mA_n^*B_p^*)[\mathrm{sinc}((\gamma_l-\gamma_m+\gamma_n-\gamma_p)L_z/2)$$
$$-(A_lB_mB_n^*B_p^*+B_lA_mA_n^*A_p^*)[\mathrm{sinc}((\gamma_l-\gamma_m+\gamma_n+\gamma_p)L_z/2)] \quad \text{(B38)}$$

where $A_n = A_n(\mathrm{r};\Omega)$, $B_n = B_n(\mathrm{r};\Omega)$, $A_p = A_p(\mathrm{r};\ \omega_{p,n,q})$, and $B_p = B_p(\mathrm{r};\omega_{p,n,q})$. Also ξ_{nx}, ξ_{ny}, and γ_n are evaluated at Ω, while ξ_{px}, ξ_{py}, and γ_p are evaluated at $\omega_{p,n,q}$. Due to modal orthogonality, the quadruple modal sum in Eq. (B37) reduces to a triple sum, $\sum_l\sum_m\sum_n\sum_p U_q^{l,m,n,p}(\omega_{m,l,q},\omega_{p,n,q},v_q) = \sum_l\sum_m\sum_p U_q^{l,m,p}(\omega_{m,l,q},\omega_{p,n,q},v_q)$. Further, following the reasoning of Ref. 22, Sec. IV B, Eq. (68), terms with $m \neq p$ are negligible compared to terms for which $m = p$ as long as the size of the resolution footprint is large enough, i.e.,

$$\mathrm{sinc}((\xi_{mx}-\xi_{px}))L_x/2) \ll 1, \text{ and} \quad \text{(B39a)}$$

$$\mathrm{sinc}((\xi_{my}-\xi_{py}))L_y/2) \ll 1, \quad \text{(B39b)}$$

so that $\sum_l\sum_m\sum_p U_q^{l,m,l,p}(\omega_{m,l,q},\omega_{p,l,q},v_q) \approx \sum_l\sum_m U_q^{l,m,l,m}(\omega_{m,l,q},\omega_{m,l,q},v_q)$. An illustrative example for the length scales necessary for the above conditions to hold is presented in Fig. 9 for the waveguide of Fig. 2 and the source signal and remote sensing system parameters of Table II. We assume the targets are stationary and uniformly distributed over all depths, and that the mean range to the targets is 30 km. While the exact "necessary" length scale will differ depending on the exact modal decomposition of the field, we may still conclude that the higher the frequency and the number of propagating modes, the larger the length scale required for the double sum approximation stated above to be valid.

Under these conditions, Eq. (B37) simplifies to

$$\langle\Phi_{s,q}(\mathrm{r},t;\Omega)\Phi_{s,q}^*(\mathrm{r},t+\tau;\Omega)\rangle$$
$$= 16\pi^2\int\sum_l\sum_m \frac{|S(\omega_{m,l,q})|^2}{|k(\omega_{m,l,q})|^2}U_q^{l,m,l,m}(\omega_{m,l,q},\omega_{m,l,q},v_q)$$
$$\times e^{iv_q[\xi_l(\Omega)+\xi_m(\Omega)]\tau}e^{i\Omega\tau}\mathrm{d}v_q. \quad \text{(B40)}$$

b. Statistical moments of the ambiguity function

For a broadband source with source function $Q(\Omega) \iff q(t)$, we can use Fourier synthesis to write the scattered field and its spectrum as

$$\Psi_{s,q}(\mathrm{r},t)=\frac{1}{2\pi}\int \mathrm{d}\Omega Q(\Omega)\Phi_{s,q}(\mathrm{r},t;\Omega), \tag{B41}$$

$$\Psi_{s,q}(\mathrm{r},\omega')=\int \mathrm{d}t e^{i\omega' t}\Psi_{s,q}(\mathrm{r},t)\ . \tag{B42}$$

The expected values of $\Psi_{s,q}(r,\omega')$, and $|\Psi_{s,q}(\mathrm{r},\omega')|^2$ can then be calculated in a manner similar to the process described in Appendix B 1 b for the free-space case. The expressions are given below:

$$\langle\Psi_{s,q}(\mathrm{r},\omega')\rangle=2\frac{S(\omega')}{k(\omega')}\int\sum_l\sum_m Q(\omega'(1+v_q(1/v_l^G+1/v_m^G))^{-1}) \times U_q^{l,m}(\omega',v_q)P_v(v_q)\mathrm{d}v_q, \tag{B43}$$

$$\begin{aligned}\langle|\Psi_{s,q}(\mathrm{r},\omega')|^2\rangle &= 4\frac{|S(\omega')|^2}{|k(\omega')|^2}\int\sum_l\sum_m\sum_n\sum_p \\ &\times Q(\omega'(1+v_q(1/v_l^G+1/v_m^G))^{-1}) \\ &\times U_q^{l,m,n,p}(\omega',\omega',v_q) \\ &\times Q^*(\omega'(1+v_q(1/v_n^G+1/v_p^G))^{-1})P_v(v_q)\mathrm{d}v_q,\end{aligned} \tag{B44}$$

where v_l^G denotes the group velocity of the lth mode. Similarly, for the statistical moments of the ambiguity function, $\Psi_{s,q}(\tau,v)$ and $|\Psi_{s,q}(\tau,v)|^2$, we find

$$\begin{aligned}\langle\Psi_{s,q}(\tau,v)\rangle &= \frac{1}{\pi}\int_{-\infty}^{\infty}\frac{S(\omega')}{k(\omega')}Q^*(\omega'-2\pi v)e^{-i(\omega'-2\pi v)\tau} \\ &\times\int\sum_l\sum_m Q(\omega'(1+v_q(1/v_l^G+1/v_m^G))^{-1}) \\ &\times U_q^{l,m}(\omega',v_q)P_v(v_q)\mathrm{d}v_q\mathrm{d}\omega'\end{aligned} \tag{B45}$$

and

$$\begin{aligned}\langle|\Psi_{s,q}(\tau,v)|^2\rangle &= \frac{1}{\pi^2}\int_{-\infty}^{\infty}\int_{-\infty}^{\infty}\frac{S(\omega_1)}{k(\omega_1)}Q^*(\omega_1-2\pi v)\frac{S^*(\omega_2)}{k^*(\omega_2)} \\ &\times Q(\omega_2-2\pi v)e^{-i(\omega_1-\omega_2)\tau} \\ &\times\int\sum_l\sum_m\sum_n\sum_p Q(\omega_1(1+v_q(1/v_l^G \\ &+1/v_m^G))^{-1})U_q^{l,m,n,p}(\omega_1,\omega_2,v_q) \\ &\times Q^*(\omega_2(1+v_q(1/v_n^G+1/v_p^G))^{-1}) \\ &\times P_v(v_q)\mathrm{d}v_q\mathrm{d}\omega_1\mathrm{d}\omega_2\end{aligned} \tag{B46}$$

We note that the term $U_q^{l,m}$, which corresponds to the characteristic function of the random target position u_q^0, is evaluated at different wavenumbers between Eqs. (B45) and (B46). As demonstrated in Sec. II B, evaluating $U_q^{l,m}$ near base-band typically leads to the second moment of the ambiguity function dominating over the magnitude squared of its first moment.

The total field $\Psi_s(\mathrm{r},\omega')$ is given by summing over all targets, $\Psi_s(\mathrm{r},\omega')=\sum_{q=1}^N\Psi_{s,q}(\mathrm{r},\omega')$. We assume that: (i) target positions are i.i.d. random variables and (ii) target speeds are also i.i.d. It then follows that $\langle\Psi_s(\tau,v)\rangle=N\langle\Psi_{s,q}(\tau,v)\rangle$, and the expected value of the magnitude squared of the ambiguity function is given by

$$\begin{aligned}&\langle|\Psi_s(\tau,v)|^2\rangle \\ &=\sum_{q1=1}^N\sum_{q2=1}^N\frac{1}{\pi^2}\int_{-\infty}^{\infty}\int_{-\infty}^{\infty}\frac{S(\omega_1)}{k(\omega_1)} \\ &\times Q^*(\omega_1-2\pi v)\frac{S^*(\omega_2)}{k^*(\omega_2)}Q(\omega_2-2\pi v)e^{-i(\omega_1-\omega_2)\tau} \\ &\times\frac{1}{V^2}\int\int\int\int\sum_l\sum_m\sum_n\sum_p \\ &\times\Phi_{s,q1}^{l,m}(\mathrm{r},\omega_1(1+v_{q1}(1/v_l^G+1/v_m^G))^{-1},\omega_1) \\ &\times Q(\omega_1(1+v_{q1}(1/v_l^G+1/v_m^G))^{-1}) \\ &\times Q^*(\omega_2(1+v_{q2}(1/v_n^G+1/v_p^G))^{-1}) \\ &\times\Phi_{s,q2}^{n,p}(\mathrm{r},\omega_2(1+v_{q2}(1/v_n^G+1/v_p^G))^{-1},\omega_2) \\ &\times P_v(v_{q1})P_v(v_{q2})\mathrm{d}u_{q1}^0\mathrm{d}u_{q2}^0\mathrm{d}v_{q1}\mathrm{d}v_{q2}\mathrm{d}\omega_1\mathrm{d}\omega_2 \\ &=N\langle|\Psi_{s,q}(\tau,v)|^2\rangle+N(N-1)|\langle\Psi_{s,q}(\tau,v)\rangle|^2\end{aligned} \tag{B47}$$

where the last line is arrived at by considering the distinction between the $q2=q1$ terms and the $q2\neq q1$ terms. Again, the second moment of the ambiguity function for the total group of N targets consists of two terms: (i) a variance term proportional to N due to scattering from each target and (ii) a mean-squared term proportional to N^2 due to interaction of the fields scattered from different targets,[22] where the variance term typically dominates.[6]

[1] N. Levanon, *Radar Principles* (Wiley, New York, 1988), pp. 37–67.
[2] J. V. DiFranco and W. L. Rubin, *Radar Detection* (Prentice-Hall, Englewood Cliffs, NJ 1968), pp. 289–335.
[3] R. J. Doviak, D. S. Zrnic, and D. S. Sirmas, "Doppler weather radar," Proc. IEEE, **67**, 1522–1553 (1979).
[4] R. Pinkel, "Doppler sonar measurements of ocean waves and currents," Deep-Sea Res., Part A. **28**(3), 269–289 (1981).
[5] J. M. B. Dias and J. M. N. Leitao, "Nonparametric estimation of mean Doppler and spectral width," IEEE Trans. Geosci. Remote Sens. **38**(1), 271–282 (2000).
[6] M. Andrews, Z. Gong, and P. Ratilal, "High resolution population density imaging of random scatterers with the matched filtered scattered field variance," J. Acoust. Soc. Am. **126**, 1057–1068 (2009).
[7] R. Bainbridge, "The speed of swimming of fish as related to size and to the frequency and amplitude of the tail beat," J. Exp. Biol. **35**, 109–133 (1958).
[8] F. J. Hester, "Identification of biological sonar targets from body motion doppler shifts," in *Symposium on Marine Bioacoustics*, edited by W. N. Tavolga (Pergamon Press, New York, 1967), pp. 59–74.
[9] D. V. Holliday, "Doppler structure in echoes from schools of pelagic fish," J. Acoust. Soc. Am. **55**, 1313–1322 (1974).
[10] W. D. Barber, J. W. Eberhard, and S. G. Karr, "A new time domain technique for velocity measurements using Doppler ultrasound," IEEE Trans. Biomed. Eng. **32**, 213–229 (1985).
[11] B. H. Brumley, R. G. Cabrera, K. L. Deines, and E. A. Terray, "Performance of a broad-band acoustic Doppler current profiler," IEEE J. Ocean. Eng. **16**, 402–407 (1991).
[12] D. A. Demer, M. Barange, and A. J. Boyd, "Measurements of three-dimensional fish school velocities with an acoustic Doppler current profiler," Fish. Res. **47**, 201–214 (2000).
[13] L. Zedel and T. Knutsen, "Measurement of fish velocity using Doppler sonar," in *Proceedings Oceans* (2000), pp 1951–1956.
[14] Y. Lai and N. C. Makris, "Spectral and modal formulations for the Doppler-shifted field scattered by an object moving in a stratified medium," J. Acoust. Soc. Am. **113**, 223–244 (2003).

[15]Y. Lai and N. C. Makris, "Estimating the velocity of a moving object submerged in an ocean waveguide with active sonar," J. Acoust. Soc. Am. **112**, 2407 (2002).
[16]N. C. Makris, P. Ratilal, D. T. Symonds, S. Jagannathan, S. Lee, and R. W. Nero, "Fish population and behavior revealed by instantaneous continental shelf-scale imaging," Science **311**, 660–663 (2006).
[17]I. Huse and E. Ona, "Tilt angle distribution and swimming speed of overwintering Norwegian spring spawning herring," ICES J. Mar. Sci. **53**, 863–873 (1996).
[18]O. A. Misund, A. Ferno, T. Pitcher, and B. Totland, "Tracking herring schools with a high resolution sonar. Variations in horizontal area and relative echo intensity," ICES J. Mar. Sci. **55**, 58–66 (1998).
[19]D. M. Farmer, M. V. Trevorrow, and B. Pedersen, "Intermediate range fish detection with a 12-kHz sidescan sonar," J. Acoust. Soc. Am. **106**, 2481–2490 (1999).
[20]S. Jagannathan, I. Bertsatos, D. Symonds, T. Chen, H. T. Nia, A. D. Jain, M. Andrews, Z. Gong, R. Nero, L. Ngor, M. Jech, O. Godo, S. Lee, P. Ratilal, and N. Makris, "Ocean acoustic waveguide remote sensing (OAWRS) of marine ecosystems," Mar. Ecol.: Prog. Ser. **395**, 137–160 (2009).
[21]N. C. Makris, P. Ratilal, S. Jagannathan, Z. Gong, M. Andrews, I. Bertsatos, O. R. Godø, R. W. Nero, and J. M. Jech, "Critical population density triggers rapid formation of vast oceanic fish shoals," Science **323**, 1734–1737 (2009).
[22]P. Ratilal and N. C. Makris, "Mean and covariance of the forward field propagated through a stratified ocean waveguide with three-dimensional random inhomogeneities," J. Acoust. Soc. Am. **118**, 3532–3559 (2005).
[23]T. H. Glisson and A. P. Sage, "On sonar signal analysis," IEEE Trans. Aerosp. Electron. Syst. **AES-6**, 37–50 (1969).
[24]T. Collins and P. Atkins, "Doppler-sensitive active sonar pulse designs for reverberation processing," IEEE Proc., Radar Sonar Navig. **145**, 347–353 (1998).
[25]S. Haykin, B. Currie, and T. Kirubarajan, "Adaptive radar for improved small target detection in a maritime environment," Technical Report 03-01, DRDC Ottawa, 2003.
[26]A. P. Dowling and J. E. F. Williams, *Sound and Sources of Sound* (Horwood, Chichester, 1983), pp. 187–189.
[27]H. P. Bucker and H. E. Morris, "Normal-mode reverberation in channels or ducts," J. Acoust. Soc. Am. **44**, 827–828 (1968).